

# **SUPERIONIC CONDUCTIVITY IN ION - EXCHANGED LITHIUM - CONTAINING GLASSES**

**A Thesis Submitted  
In Partial Fulfilment of the Requirements  
for the Degree of**

**MASTER OF TECHNOLOGY**

**by  
ASHOK KUMAR**

*to the*  
**INTERDISCIPLINARY PROGRAMME IN MATERIALS SCIENCE  
INDIAN INSTITUTE OF TECHNOLOGY KANPUR**

**DECEMBER, 1987**

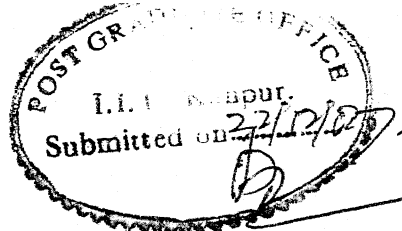
1987-13-1003  
CENTRAL LIBRARY  
Kanpur.

Acc. No. **A**...99742

Thesis  
680/1287  
Ac 562

1987-M-KUM-SUP

*Dedicated to  
My Parents*



# CERTIFICATE

This is to certify that the thesis entitled 'SUPERIONIC CONDUCTIVITY IN ION-EXCHANGED LITHIUM-CONTAINING GLASSES' being submitted by Mr. Ashok Kumar, in partial fulfilment of requirements for the award of an M.Tech. degree in Materials Science Programme, to the Indian Institute of Technology, Kanpur is carried out by him under our supervision and has not been submitted for the award of any other degree or diploma elsewhere.

Date : December 14 , 1987.

*K. Shahi*

( K. Shahi. )  
Assistant Professor

*D. Chakravorty*

( D. Chakravorty )  
Professor

Materials Science Programme  
Indian Institute of Technology,  
Kanpur

## ACKNOWLEDGEMENTS

I owe an enormous debt of gratitude to Professor D. Chakravorty who introduced me to the subject of glass science, for his consistent guidance, inspiration, encouragement and full freedom throughout the course of the present work. I am equally deeply indebted to Dr. K. Shahi for his keen discussions, active participation and lively suggestions on the subject.

I am further grateful to all faculty and staff members of this department who extended their help whenever needed.

I sincerely thank Mr. B. Sharma for his courteous co-operation and help in the experimental part of the present work.

I also express my thanks to all my friends and colleagues who constructively contributed to the cause of this work directly or indirectly.

It is a great pleasure to place on record the financial assistance received from the "Council of Scientific and Industrial Research" through fellowship no. ( renewed) 9/92/(30)/86-EMR-I.

Ashok Kumar .

## CONTENTS

	PAGE
Acknowledgements	
List of Figures	iii
List of Tables	v
Synopsis	vi
CHAPTER 1 INTRODUCTION	1
1.1.1 Superionic conductors and solid electrolytes	2
1.1.2 Fast ion conducting glasses	4
1.2 Electrical conduction in glasses	5
1.2.1 Electronic conduction	5
1.2.2 Transport	9
1.2.3 Materials	10
1.2.3.1 Elemental and chalcogenide glasses	10
1.2.3.2 Transition metal oxide glasses	12
1.2.4 Electronic switching	13
1.3 Ionic conduction in glasses	13
1.3.1 Ionic conductivity-Electrode Polarization	17
1.3.2 Compositional effects on ionic conductivity	19
1.4 Glass transition	20
1.5 Ion exchange	21
1.6 Statement of the problem	22

CHAPTER 2	EXPERIMENTAL TECHNIQUES	24
2.1	Preparation of glass	24
2.2	Sample preparation for electrical characterization	24
2.3	D.C. Resistivity measurements	27
2.4	A.C. Resistivity measurements	27
2.5	Sample preparation for ion-exchange	30
2.6	X-ray analysis	31
2.7	Differential thermal analysis	31
2.8	Blocking electrode measurements	32
CHAPTER 3	RESULTS AND DISCUSSION	34
3.1	X-ray analysis	34
3.2	Differential thermal analysis	37
3.3	Density measurements	37
3.4	Electrical measurements	37
3.4.1	A.C. Measurements	39
3.4.2	D.C. Measurements	44
3.4.3	Discussion	50
3.5	Polarization measurements	60
3.5.1	Discussion	68
CHAPTER 4	CONCLUSION AND FUTURE SCOPE OF WORK	69
REFERENCES		71

## LIST OF FIGURES

Figure No.		Page
1.1	A true gap in the density of states with some band tailing	7
1.2	Cohen-Fritzche-Ovshinsky model of overlapping valence and conduction band tails	7
1.3	The energy configuration in a glass	7
2.1	Schematic view of the conductivity cell	26
2.2	Schematic representation of the mor- phology of the ion-exchanged sample	28
2.3	Schematic circuit diagram for DC resistivity measurements	28
3.1	X-ray diffraction pattern for glass system G1	36
3.2	X-ray diffraction pattern for glass system G2	36
3.3	X-ray diffraction pattern for glass system ( High conducting state) HIG2	36
3.4	Differential thermal analysis curve for glass system G1	38
3.5	Differential thermal analysis curve for glass system G3	38
3.6	Differential thermal analysis curve for glass system G5	38
3.7	Complex impedance plot for glass system G1	40
3.8	Complex impedance plot for ion-exchanged glass system IG2	40
3.9	Complex impedance plot for ion-exchanged glass system. IG1	41
3.10	Complex impedance plot for glass system G2	42
3.11	Complex impedance plot for glass system G3	43
3.12	Temperature variation of DC resistivity for glass systems G1, IG1 and HIG1.	45



3.13	Temperature variation of DC resistivity for glass systems G2, IG2 and HIG2	46
3.14	Temperature variation of DC resistivity for glass systems G3, IG3 and HIG3	47
3.15	Temperature variation of DC resistivity for glass systems G4, IG4 and HIG4	48
3.16	Temperature variation of DC resistivity for glass systems G5, IG5 and HIG5	49
3.17	Switching of glass system IG3 ion-exchanged at 330°C to HIG3 state	51
3.18	Switching of glass system IG1 ion-exchanged at 330°C to HIG1 state	51
3.19	Switching of glass system IG2 ion-exchanged at 330°C to high conducting state HIG2	52
3.20	Switching of glass system IG4 ion-exchanged at 330°C to high conducting state HIG4	53
3.21	Switching of glass system IG5 ion-exchanged at 330°C to high conducting state HIG5	54
3.22	Current-voltage characteristics for polarization cell Ag/HIG1/C <sup>+</sup>	61
3.23	Current-voltage characteristics for Ag/HIG2/C <sup>+</sup> polarization cell	61
3.24	Current-voltage characteristics for polarization cell Ag/HIG3/C <sup>+</sup>	62
3.25	Current-voltage characteristics for polarization cell Ag/HIG4/C <sup>+</sup>	62
3.26	Current as a function of time for system Ag/HIG1/C <sup>+</sup>	63
3.27	Current as a function of time for system Ag/HIG2/C <sup>+</sup>	64
3.28	Current as a function of time for system Ag/HIG3/C <sup>+</sup>	64
3.29	Current as a function of time for system Ag/HIG4/C <sup>+</sup>	66
3.30	Temperature variation of electric field (E <sub>c</sub> ) for glass systems IG1 and IG2	67

## LIST OF TABLES

TABLE No.		PAGE NO.
3.1	Composition of Glass Systems	35
3.2	Density and Glass Transition Temperatures of Glass Systems	35
3.3	Activation Energy and Pre- exponential Factors for Composition No. 1	55
3.4	Activation Energy and Pre- exponential factors for Composition No. 2	55
3.5	Activation Energy and Pre- exponential Factors for Composition No. 3	55
3.6	Activation Energy and Pre- exponential Factors for Composition No. 4	56
3.7	Activation Energy and Pre- exponential Factors for Composition No. 5	56

## SYNOPSIS

There have been several detailed studies reported in the literature of ionic conductivity in oxide glasses particularly silicate glasses and aluminasilicate glasses containing significant concentrations of alkali ions. In the present work we have explored the effect of lithium ion content on the conductivity of some silica based glasses both in virgin and  $\text{Li}^+ \rightleftharpoons \text{Ag}^+$  ion exchanged states in an effort to optimize the structure and composition for possible application as solid electrolytes. Both a.c. and d.c. resistivity measurements of certain silicate glass compositions containing 10-30 mol %  $\text{Li}_2\text{O}$  and subjected to  $\text{Li}^+ \rightleftharpoons \text{Ag}^+$  ion-exchange treatment in the bulk form have been made. The polarization ( blocking electrode) measurements have been made to ensure that the conduction is essentially ionic in nature.

The ion-exchanged samples exhibit resistivity and activation energy values lower than those of virgin (non ion-exchanged) samples. A suitable combination of electric field and temperature brings about a further semipermanent reduction in resistivity and activation energy values. The typical values of resistivity and activation energy in this high conducting state are 50 ohm-cm and 0.04 eV respectively. Such behaviour is explained on the basis of formation of an interconnected silver rich phase under the combined influence of temperature and suitable electric field. The conductivities exhibited by these materials are comparable to the conductivities exhibited by some of the conventional fast ion conducting glasses containing

a higher silver concentration than those incorporated in the present glass systems by an ion exchanged process.

Chapter I deals with the brief review of theory of electrical conduction ( both electronic and ionic) in glasses. Compositional and electrode polarization effects on ionic conductivity are followed by a brief review of ion exchange process. In the end the purpose and statement of our problem have been stated.

Chapter II describes the experimental parts involved in the present work. The preparation and characterization methods of glass samples are discussed. The characterization techniques include a.c. and d.c. resistivity measurements and differential thermal analysis (DTA) .

In Chapter III results obtained in the present investigation have been presented. The results of a.c. and d.c. resistivity, X-ray, DTA, Polarization and density measurements of certain silicate glass composition containing 10-30 mole %  $\text{Li}_2\text{O}$  both in virgin and  $\text{Li}^+ \rightarrow \text{Ag}^+$  ion-exchanged ( in the bulk form) have been presented. The various results obtained have been discussed and plausible explanation for them have been given.

In the last chapter IV the conclusion of present work has been given and the scope of future work in this field of research has been suggested.

## CHAPTER 1

### INTRODUCTION

Glass is a material of great technical importance. It functions equally well as a carrier of light, protector of man and his inventions, an object of art, or an indispensable tool for the exploration of science. Depending upon composition it can be made stronger than steel ( Charles 1961) or soluble in water, a detector of nuclear radiations ( Kreidl 1956) or the source of powerful laser beam (Snitzer 1967). Certain compositions are known to have either negative, zero or positive thermal expansion co-efficients. Some compositions are colorless, black or selective in their light transmission properties (Cohen, Armistead 1964, Smith). Paramagnetic and diamagnetic glasses can also be made depending upon the choice of composition. The electrical conductivities can vary from  $10^{-3}$ - $10^{-18}$   $\text{Ohm}^{-1}\text{Cm}^{-1}$  with either electronic or ionic type of conduction mechanism or a combination thereof being present. It is essentially the electrical properties that we are mainly concerned with in the present studies of silicate glasses containing 10-30 mole%  $\text{Li}_2\text{O}$ .

The electrical properties of glasses provide interesting opportunities for studying glass structure. It has been well known for several years that electrical properties of oxide glasses containing significant contribution of alkali ions

such as  $\text{Na}^+$  are dominated by alkali ion motion within the glass network. In fact ionic transport has been the subject of study since 1984 when Warburg showed that sodium can be transported through thuringer glass from one sodium- amalgam bath to another by the application of a D.C. voltage across the glass envelop. There has been several detailed studies of ionic conductivity in network forming glasses particularly silicate glasses ( Charles 1963) and aluminosilicates ( Isard 1959) containing alkali modifiers but the best conductivities achieved are about  $10^{-7} \text{ Ohm}^{-1} \text{ Cm}^{-1}$  at room temperature and  $10^{-4} \text{ ohm}^{-1} \text{ cm}^{-1}$  at 500K. These values are too low for the majority of applications concerning energy devices.

#### 1.1.1 SUPER IONIC CONDUCTORS AND SOLID ELECTROLYTES :

The vast majority of new materials which have emerged in the recent years for application as solid electrolytes have been crystalline materials the so called superionic solids in which structure allows fast ion motion along certain crystallographic directions. Though the conductivities of solid electrolytes are comparable with those of liquid electrolytes but they have distinct advantages over liquid electrolytes which are the following:

- (i) No need for container
- (ii) Very high energy and power handling capacities.
- (iii) Longer shelf life
- (iv) High ruggedness
- (v) Wide temperature range of operation.

5

The microscopic mechanism for ionic conduction can be understood in terms of hopping of mobile ions between neighbouring interstitial sites within the structure. Optimum materials have a high density of mobile ion species, a high density of vacant interstitial sites and a low potential barrier for ionic motion between sites. This latter requirement implies a weak bonding of mobile ion with structural framework as well as sufficiently large channels linking mobile ion sites.

With these requirements in mind it is now worthwhile to re-examine the ionic conductivity of non-crystalline solids. These materials have the necessary degree of disorder and can be prepared with great flexibility of composition. Thus it remains to design a glass framework which allows relatively unimpeded motion of ions throughout the structure. The increased disorder of a glass over crystal of the same composition is usually associated with a decreased electronic conductivity due to decreased overlap of neighbouring electronic states. The disorder also imposes a distorted co-ordination geometry which is less formidable with covalent bonding thereby forming an increased ionic mobility. Thus these general properties point to higher ionic transference number in glasses.

From practical stand point the electric properties of glasses are isotropic unlike crystalline solids, thereby avoiding the problem associated with grain boundaries in crystalline ceramics. Most importantly it has been found that in nearly

all cases examined the glasses exhibit greater ionic conductivity than their crystalline counterparts. This has been found to be the case for silver ion ( Minami et. al. 1977), halide ion ( Leroy et. al 1978), alkali ions ( Levasseur et al 1978), sulphates (Smedley et. al. 1978) and oxides (Glass et. al. 1978) conducting glasses. However it is not possible to extend this comparison to the superionic conductors such as Na- $\beta$ -alumina since glasses of these compositions have not yet been successfully made.

### 1.1.2 FAST ION CONDUCTING GLASSES :

The concept that some of the best crystalline solid electrolytes like  $\alpha$ -AgI (Shahi 1977) and  $\beta$ - $\text{Al}_2\text{O}_3$  ( Yao and Kummer 1967, Sudworth 1984) involve open channel structure and high degree of disorder of the mobile ions, has prompted investigations of glassy solid electrolytes ( Tuller et. al. 1980). The significant development in rapid quenching techniques has resulted in production of alkali meta-niobates and meta-tantalate glasses having conductivities many orders of magnitudes higher and fairly low activation energy (0.4 eV) than corresponding crystalline phases. Greater plasticity, isotropic conductivity and absence of grains are distinct advantages of fast ion conducting glasses over crystalline superionic solids.

Most of the fast ion conducting (FIC) glasses are based on composition derived from AgI which itself is a fast ion conductor in crystalline form. Highest conductivity is exhibited by FIC glasses based on silver ion migration. Very few of the FIC's are



based on  $\text{SiO}_2$  as network former because of the problem of silver precipitating out as metallic silver agglomerates during the melting process (Reibling 1971). Large concentrations of silver ions in silica based glasses has been, however, achieved (Frischat 1976) by subjecting glass fibres to alkali ions. Silver ion exchange treatment at a temperature well below the glass transition temperature. This work has been lucidly reported by Chakravorty and Srivastava (1972). The silver rich layers produced by an ion exchange reaction are usually only a few tens of micrometers thick (Collins et.al. 1966).

In the following section we briefly review the theory of electrical conduction in glasses both electronic and ionic type of conductivities alongwith their mechanism.

## 1.2. ELECTRICAL CONDUCTION IN GLASSES :

In order for a current to flow in a glass, charge must somehow be transported. Electrons may move through the system in one of the two ways. Either by moving with nuclei in which case ionic conductivity occurs, or by becoming detached from one atom and moving to another, in which case electronic conductivity is present. It is also possible of course that both the ionic and electronic processes occur simultaneously. The transfer number  $T_x = \sigma_x / \sigma_T$  expresses the fraction of total conductivity contributed by each type of charge carriers.

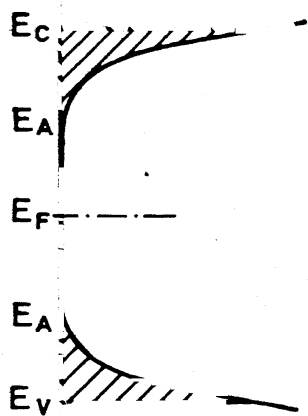
### 1.2.1 ELECTRONIC CONDUCTION :

Though in the present work we are not mainly concerned with

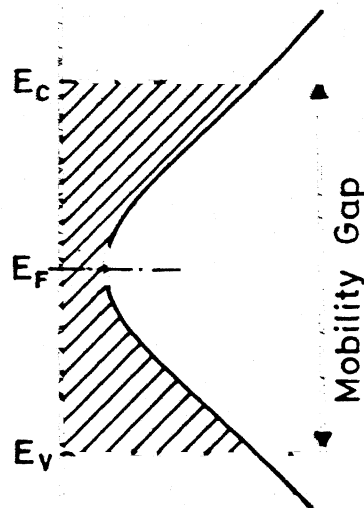
the electronic conduction as such, yet since it is always present, though masked by ionic conduction in silica based glasses and certain other amorphous materials and still other crystalline materials the so called superionic solids, and in certain classes of materials like chalcogenide glasses and transition metal oxide glasses it is the electronic conduction which dominates, the brief review of theory of electronic conduction in glasses is inevitable.

Every transparent material must of course be associated with a band structure. However the nature of bandgap in crystalline and amorphous material is not the same. The presence of disorder in amorphous materials causes the tailing of states into gap at the band edges ( Mott 1979). The potential fluctuation in short range order, such as bond angle distortions, leads to tailing of states in the band gap ( Fig. 1.1).

Another cause of band tailing can be the occurrence of short-range disorder in non-bonded atom distances. This is particularly important for chalcogen atoms ( Group IV elements) which have one non-bonding p-like orbitals ( forming the top of valence band), in addition to two predominantly P like bonding orbitals per atom. If two such atoms are forced close to each other in the random network the interaction between the non-bonding lone-pair orbitals causes the energy of such states to be raised, again producing tailing of states from the valence band edge into the gap. The result of all these effects gives rise to the Cohen-Fritzsche-Ovshinsky 1969, model for density of



N(E)



N(E)

Fig. 1.1 A true gap in the density of states with some band tailing.

Fig. 1.2 Cohen-Fritzsche-Ovshinsky model of overlapping valence and conduction band tails.

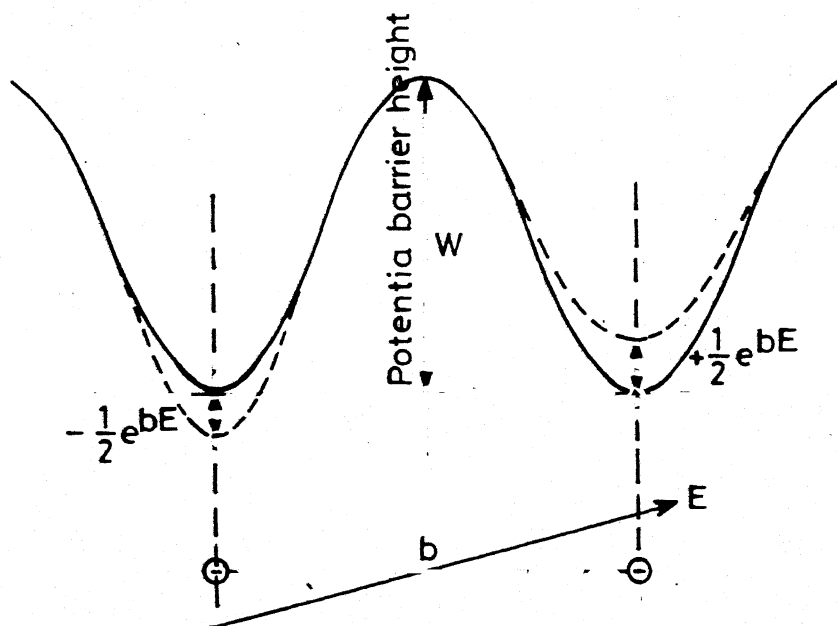


Fig. 1.3 The energy configuration in a glass. Solid lines indicate energy without field. Dashed lines indicate energy with applied electric field.

states in the gap of an amorphous multicomponent chalcogenide semiconductor ( Fig. 1.2). In this, the band tailing is so pronounced that the tails arising from the valence and conduction bands actually overlap in the midgap.

The important point about the states in gap, which are the consequence of disorder, is that the electrons may become localised i.e. spatially confined to the vicinity of predominantly a single atomic site. The occurrence is more probable the greater the degree of disorder in the potential experienced by the electrons, and so is more likely in the band tails, since these arise in general from the most distorted sites. The estimation of degree of disorder necessary to localize, say, all states in the band, having at our disposal means of distinguishing between localized and extended states will not be discussed here and can be referred to as in some book dealing with amorphous semiconductors.

For a particularly useful example let us consider the case of Ge (Grigorovici, 1969). Starting with a perfectly periodic structure in which all states are the normal band states with clean band-gap. As a small amount of disorder is introduced, the number of band states decreases and localized states are formed having energies at the top and bottom of the band. As the amount of disorder increases more states are split off from the band and form localized states. Finally if the disorder is sufficient, all states will be localised ( Anderson 1958).

## 1.2.2 TRANSPORT :

We now consider the problem of transport in a disordered lattice. Three regions have been recognized (a) band conduction as in crystalline materials for electrons with energy greater than the conduction band edge since such electrons have extended wave functions (b) thermally activated hopping among localized states for electrons below conduction band edge, and (c) a diffusion mechanism for electrons with energy just above conduction band edge (Anderson 1958).

Coming under close scrutiny amorphous solids have been found to obey in some cases, physical laws quite distinct from those of crystalline solids. Particularly notables are Mott's  $\exp(T^{-1/4})$  conductivity law for some amorphous semiconductors at low temperature and linear heat capacity of many glasses at low temperatures.

The most important mechanism which seem to occur in a glass material is the one due to hopping. This may be understood by considering a localised electron on one site and second site nearby having a slightly different energy. For the electron to hop it will need to gain or loose energy from thermal vibrations. A second hopping region may exist if the sites are extremely close together. Then the electrons may desire to localize itself on two sites with the lattice polarization then surrounding both the sites.

For hopping of an electron between two sites, we find that the transition rate will increase as the sites come closer

together. The transition rate increases exponentially with activation energy for transition also increasing. If the binding energy is small, this increase may not come until quite high temperatures. Finally in the high temperature region, the activation energy will be smaller for closer sites than for more distant sites.

### 1.2.3 MATERIALS :

There is no agreement at present time as to the conduction mechanism in amorphous materials. Indeed different experiments appear to give conflicting results. One aspect, common to most amorphous material is that the conductivity is insensitive to small amounts of cation impurities ( several percent), in marked contrast with the situation in crystalline semiconductors, where impurities, in parts per million range, cause orders of magnitude change in the conductivity. This is frequently attributed to the ability of amorphous materials to satisfy the bond requirements of the impurities ( Mott. 1967). It may also be a result of the effects of the impurities being swamped by defects produced by the amorphous state.

The most frequently studied amorphous materials which exhibit semiconducting properties fall into one of the three categories

#### 1.2.3.1 ELEMENTAL AND CHALCOGENIDE GLASSES :

The elemental glasses include mainly Ge, Si, As, Te, C, B, Sb and Se ( Davis and Shaw 1970) and the chalcogenide glasses include

compounds containing group VI elements such as S, Se and/or Te (Pearson 1964). The glasses based on cadmium arsenide probably also belongs to this category because of their similar behavior. The d.c. conductivity expression for these material is given by :

$$\sigma = \sigma_0 \exp ( - Q/kT ) \quad \dots \quad (1.1)$$

where  $\sigma_0$ , the pre-exponential factor and  $Q$ , the activation energy, are temperature dependent parameters.

The high temperature d.c. conductivity in elemental and chalcogenide glasses is attributed mainly to the excitation of carriers across the forbidden gap. In amorphous Ge and Si the measured activation energy drops with decreasing temperature. This drop is generally attributed to the hopping of carriers in localized states near the centre of the gap. These states arise from the overlap in the localized tails from the top of the valence band and bottom of the conduction band.

The a.c. conductivity in the elemental and chalcogenide glasses in which cases it has been comprehensively investigated is found to have two regions, one proportional to  $\omega$  and the other at higher frequencies to  $\omega^2$ , where  $\omega$  is the frequency.

In chalcogenide glasses conduction has been described as occurring in an energy band as in crystalline semiconductors ( Mott 1969 ). Fritzsche has proposed a heterogenous model which states that the regions in which mostly holes are localized are

different from regions in which electrons are localized. He proposed that there are three kinds of electronic states: Those localized in regions, channel states that extends through the material, but are excluded from certain regions and extended states for which electrons have a finite probability of appearing anywhere in the material. A random phase model of conduction band has also been proposed by Hindley (1971).

#### 1.2.3.2 TRANSITION METAL OXIDE GLASSES:

They include in particular the oxides of vanadium, titanium and iron (Mackenzie). The semiconductivity of these glasses is generally considered to arise due to hopping of carriers for one strongly localized state to another. The two states are the two valence states of the transition metal ion. However there is little agreement as to whether the conduction in these glasses is by normal band conduction or by motion of a polaron (Adler 1968).

The conductivity for these glasses is given by (Mott 1968, Austin and Mott 1969):

$$\sigma = \frac{\mu_{ph} e^2 c(1-c)}{kTR} \exp(-2\alpha_{\omega} R) \exp\left[\frac{-E_H + E_0}{2kT}\right] \quad (1.2)$$

where  $\mu_{ph}$  is the phonon frequency,  $c$  is the ratio of the concentration of the ions in lower valency to the total concentration of the transition metal ions,  $\alpha_{\omega}$  is the rate of decay of wave function,  $R$  is the average hopping distance,  $E_H$  is the polaron hopping energy and  $E_0$  is the energy disorder.



#### 1.2.4 ELECTRONIC SWITCHING:

The switching devices that use amorphous semiconductors are much simpler in structure, easy to fabricate, more versatile in performance and cheaper to produce than their crystalline counterparts. The greatest attribute of these devices is their capability to display memory switching in addition to threshold switching which cannot be achieved by any of the existing devices using crystalline semiconductors.

Basically switching consists of a transition from a state of high resistance (OFF) to one of low resistance (ON), the transition being generated by the application of a specific voltage named threshold voltage  $V_{th}$ . The difference in the threshold switching and memory switching lies in the fact that in the latter, once the current is suppressed the state of low resistance still remains. In other words, no holding voltage is required once the device is switched ON. It will remain in its ON state till another reset pulse is applied to change its state from ON to OFF. This effect has been explained on the basis of formation of crystalline filament which forms because of the joule heating of the amorphous material (Tanaka et. al. 1970).

#### 1.3 IONIC CONDUCTION IN GLASSES :

Ionic conduction is well known in crystalline solids (Salamon 1979, Chandra 1981), and both cations and anions can carry currents in certain circumstances. Materials are called super-ionic materials with conductivities comparable with that

of liquid electrolytes ( $\sim 10^{-1} - 10^{-4} \Omega^{-1} \text{cm}^{-1}$ ), the mechanism giving rise to the (super)-ionic conduction may be either of the point defect or the molten sublattice type, in the former, transport is through thermally generated frenkel or Schottky defect pairs and conduction is therefore thermally activated, in the latter the number of ions of a particular type is less than the number of available sites in their sublattice and therefore a large number of ions are able to conduct with lower activation energy than for the defect process.

Although in many non-metallic amorphous solids current is carried by electrons, discussed in section 1.2.1, in others containing a relatively large proportion of ions, particularly ionic conduction may make a significant, even dominant, contribution to the total conductivity. Since many glasses based particularly around the silicate compositions, often do contain a large amount of alkali ions, the likelihood of ionic conduction is obviously quite high, and we will therefore discuss this important form of conduction in what follows.

The ionic conductivity results from the long range migration of charge carriers through the glass network under the driving force of an applied electric field. A simple expression for the ionic conductivity may be derived by assuming that the ionic motion occurs by field enhanced thermally activated hopping between vacant sites in the disordered lattice. The action of the applied electric field  $E$  is to lower the energy of a site by an amount equal to  $qEa$ , where  $q$  is the charge of the ion and  $a$  is the intersite spacing.

Consider the ion movement in one dimension jumping over the potential barrier  $W$  (Fig. 1.3). The probability  $P$  that an ion will move to either the right or left is  $P = \alpha \frac{kT}{h} \exp \frac{-W}{kT}$  where  $\alpha$  is accommodation co-efficient related to the irreversibility of the jump,  $\frac{kT}{h}$  is the vibrational frequency of the ion in the well. When electric field  $E$  is applied the potential barrier to the ion motion is slightly shifted. The field will lower the potential barrier on the side in the direction of the field and raise it on the other side by an equivalent amount. If the distance between the two wells is  $b$  the potential on the right side will now be smaller by an amount  $\frac{1}{2} ZeEb (= \frac{1}{2} Fb)$ , where  $ZeE = F$ , force on the ion and  $Z$  is the valence of the ion. Therefore the probability of the motion to the right as per the Figure (1.3) .

$$P^+ = \frac{1}{2} \alpha \frac{kT}{h} \exp - \frac{[W - \frac{1}{2} Fb]}{kT}$$

$$\text{or } P^+ = \frac{1}{2} P \exp \frac{Fb}{2kT} \quad \dots \quad (1.3)$$

and the probability of the motion to the left ( Fig. 1.3)

$$P^- = \frac{1}{2} \alpha \frac{kT}{h} \exp \frac{-(W + \frac{1}{2} Fb)}{kT}$$

$$\text{or } P^- = \frac{1}{2} P \exp \frac{-Fb}{2kT} \quad \dots \quad (1.4)$$

Consequently the positive transition will be more frequent than the negative and there will be an average drift velocity to the right in the field direction. The mean velocity of the drift

motion is:

$$\bar{V} = b(P^+ - P^-) = \frac{1}{2} bP \left[ \exp \frac{Fb}{2kT} - \exp \frac{-Fb}{2kT} \right]$$

$$\bar{V} = bP \sinh \frac{Fb}{2kT} \quad \dots \quad (1.5)$$

From the above result as long as the field strength is much smaller than  $kT$  i.e.  $\frac{1}{2} Fb \ll kT$  then  $\sinh$  can be replaced by the argument and the drift velocity can be expressed as:

$$\bar{V} = \frac{b^2 PF}{2kT} \quad \dots \quad (1.6)$$

In other case where very large field strengths exists, the first term in  $\sinh$  will dominate and  $\bar{V} = \text{Constt.} \exp \frac{bF}{2kT}$ .

At room temperature  $bF$  is small compared with  $kT$  upto field strengths of  $10V/Cm$ . Therefore the current will be proportional to the field strength in agreement with the Ohm's Law.

$$J = nZe\bar{V} = nZe \frac{b^2 PF}{2kT} = \frac{nz^2 e^2 b^2 PE}{2kT} \quad \dots \quad (1.7)$$

where  $q = Ze$ ,  $n$  = no. of ions/cc and substituting.

$$P = \alpha \frac{kT}{h} \exp \frac{-W}{kT} \quad \text{and} \quad W = \frac{\Delta F_{dc}}{N}$$

where  $\Delta F_{dc}$  is the change in free energy for dc conduction in Kilo-calories per mole and  $N$  is Avagadro number ( $6.023 \times 10^{23}$ )

$$\text{so } J = \frac{n z^2 e^2 b^2 E}{2h} \exp \left( \frac{-\Delta F_{dc}}{RT} \right) \quad \dots \quad (1.8)$$

Therefore the electrical resistivity of the glass:

$$R = \frac{E}{J} = \frac{2h}{n^2 z^2 e b^2} \exp + \frac{\Delta F_{dc}}{RT}$$

$$\text{or } \log R = \log \frac{2h}{n^2 z^2 e b^2} + \frac{\Delta F_{dc}}{RT} \quad \dots (1.9)$$

which is identical to  $\log \rho = A + \frac{B}{T}$ . A variety of glass systems are known to behave according to this equation.

### 1.3.1 IONIC CONDUCTIVITY - ELECTRODE POLARIZATION :

Ion transport within the glass under a dc potential eventually leads to the build up of the charge at the glass electrode interface if the ions are not replenished at the electrode. This phenomenon is termed electrode polarization and it can drastically affect the magnitude of dc conductivity measured. Three regions of ionic conductivity are generally seen when conductivity of a typical silicate glass is plotted versus time when a fixed dc voltage ( $\sim 1V$ ) is applied to the sample.

At very short times conductivity increases due to various dielectric contributions. At very long time intervals the conductivity decreases indefinitely owing to the fact that the mobile cations pile up at the electrodes which results in an induced back field. The back field concentrates the potential drop in the electrode region (Proctor and Sutton 1960). The back field builds up indefinitely as time progresses resulting in a continuous decrease in glass conductivity.

It is thus evident that d.c. conductivity is dependent on the time interval at which the measurement is made. At higher temperatures when the conductivity is in the range of  $> 10^{-5} \text{ ohm}^{-1} \text{ cm}^{-1}$  electrode polarization occurs so rapidly ( $\sim 10 \text{ sec.}$ ) that measurements of actual conductivity becomes quite difficult. There are three possible ways to solve the problem of accurate experimental measurement of d.c. ionic conductivity posed by electrode polarization.

1. To conduct the  $\sigma$  vs  $t$  curves at each temperature to ensure that measurements are made neither at very short time interval nor at very long time intervals.
2. It is possible to use non blocking electrodes which provide a source and sink for the mobile ions.
3. Another approach is to calculate the current flow required to produce the back potential necessary to decrease the conductivity of the glass to a given fraction of its true non-blocked value. Kinser and Hench (1969) have shown that the back potential  $\Omega_b$ , due to the polarization charge per unit area,  $q$ , is simply

$$\Omega_b = \frac{qd}{2\epsilon\epsilon_0} \quad \dots \quad (1.10)$$

where  $\epsilon$  is the permittivity of the glass,  $d$  is the thickness and  $\epsilon_0$  is the permittivity of free space. The charge  $q_b$  to form the back potential can be related to the current flow as :

$$q_b = 2 \int_0^t J dt = Jt \quad \dots \quad (1.11)$$

The current,  $J$ , required to form the back charge is directly related to the applied potential,  $V_a$ , and the conductivity of the glass, as  $J = V_a \sigma$ . With this value of  $J$  the expression of  $q_b$  becomes :

$$q_b = V_a \sigma t \quad \dots \quad (1.12)$$

### 1.3.2. COMPOSITION EFFECTS ON IONIC CONDUCTIVITY :

In nearly all investigations ( Owen. 1963, Taylor 1956, Moore and Dilva 1952, Seddon et. al. 1932) in silica based glasses with alkali ions as modifiers it has been seen that conductivity increases until a range of 20-30 mole % modifier is reached after which effect becomes progressively lesser. The range of conductivity is  $10^{-16} \text{ ohm}^{-1} \text{ cm}^{-1}$  to  $10^{-7} \text{ ohm}^{-1} \text{ cm}^{-1}$  at room temperature. The relative effect of alkali type on conductivity is  $\text{Na}^+ > \text{Li}^+ > \text{K}^+$ . The addition of only parts per million of  $\text{Na}^+$  ions is sufficient to drastically increase the conductivity of fused silica and the conductivity is directly related to the  $\text{Na}^+$  ion content ( Owen and Douglas 1959).

Substitution of  $\text{Al}_2\text{O}_3$  for  $\text{SiO}_2$  in alkali silicate glasses is very interesting ( Isard 1959). As the  $\text{Al}_2\text{O}_3$  content increases the conductivity increases and activation energy for conduction decreases. This behaviour appears to be associated with the Aluminium Ion entering the network in four fold co-ordination reducing the number of nonbridging oxygen ions. The

nonbridging oxygen co-ordination shell about the sodium ion must be decreased which could serve to increase the alkali ion mobility.

#### 1.4 GLASS TRANSITION :

The glass transition is a phenomenon in which a solid amorphous phase exhibits a more or less abrupt change in derivative thermodynamic properties ( e.g. heat capacity or thermal expansivity) from crystal like to liquid like values with change of temperature. When a liquid is cooled, it may either crystallize at the melting point or may become supercooled becoming more viscous with decreasing temperature, and may ultimately form a glass. The temperature which separates the super cooled liquid from the glass is generally taken as the glass transition temperature  $T_g$ . Although it appears that  $T_g$  defined in this way is a precise temperature, in fact this is not so, it depends on the rate of cooling of the supercooled liquid. It is found that the slower the rate of cooling, the larger is the temperature region for which the liquid may be super cooled and hence the lower is the glass transition temperature. Thus the glass transition temperature of a particular material depends upon its thermal history and is not an intrinsic property of the material. The actual value of the glass transition temperature may vary by as much as 10-20% for widely differing cooling rates. For silica based glasses, the change in  $T_g$  for different cooling rates



may be as much as 100-200K for values of  $T_g$  in the range of 600-900K. An expression relating  $T_g$  and the cooling rate  $q$  can be derived using free volume theory (Owen).

$$q = q_0 \exp \left[ -1/c (1/T_g - 1/T_m) \right] \quad \dots \quad (1.13)$$

where  $c$  and  $q_0$  are constants for the specimen.

Certain thermodynamic variables (Volume, entropy, enthalpy) are continuous through the glass transition, but exhibit a change of slope there. This implies that at  $T_g$  there should be a discontinuity in derivative variables, such as thermal expansion  $\alpha_T = (\partial \ln V / \partial T)$ , compressibility  $K_T = -(\partial^2 \ln V / \partial P) T$  and heat capacity  $C_p = (\partial H / \partial T)_p$ . This is indeed the case. The value of heat capacity shows discontinuity at  $T_g$ . Below  $T_g$  the heat capacity is considerably smaller than liquid. The above discussion suggests that the glass transition is a manifestation of second-order phase transition. Nevertheless the phenomenon of glass transition is very complex and no single theory has been advanced which is capable of accounting for all its aspects.

### 1.5 ION EXCHANGE :

Glass placed in contact with a medium containing monovalent cations, such as a fused salt or aqueous solution, can exchange monovalent ions in its matrix with the cations of the medium. An exchange cation normally has a different mobility from the original ion. Therefore as interdiffusion proceeds

one ion tends to outrun the other and an electrical potential is built up. However accompanying this change is a potential gradient that slows down the fast ions and speeds up the slow ones. To preserve the charge neutrality the fluxes of the two ions should be equal and opposite and the potential gradient ensures this in spite of the difference in the mobility of the cations.

The silver rich layers produced by an ion-exchange reaction are usually only a few tens micrometers thick (Collins et. al. 1966). The present investigation has been carried out on the bulk samples of the dimension of 2 mm each side (Fig. 2.2) using molten silver nitrate as the ion-exchange medium at temperature 330°C for 48 hours.

#### 1.6 STATEMENT OF THE PROBLEM :

As we have discussed in the previous sections that it is possible to incorporate silver ions into silicate glasses by alkali  $\rightleftharpoons$  silver ion exchange reaction at a temperature well below the glass transition temperature [ 15 ]. On ion-exchange at temperature around 330°C and duration extending to 48 hours the silver rich layer is found to be only a few tens of microns thick. Large concentrations of silver ions can be incorporated in  $\text{SiO}_2$  based glasses by subjecting the glass fibres to alkali  $\rightleftharpoons$  silver ion-exchange, glass fibres having dimensions 10 microns (Chakravorty and Srivastava 1980). Microstructural studies have revealed that the virgin glasses

have a two phase structure with the dispersed phase rich in alkali whereas after ion exchange have interconnected silver-rich phase and silver-deficient phase with disjointed interconnectivity. It has been shown that in these ion exchanged glass fibres, an optimum combination of temperature and electric field brought about a semi-permanent reduction in resistivity and activation energy values [ 7 ].

In the present work we have investigated the exchange of Li ions by Ag ions with a view to confirm the two phase microstructure in glass samples in the bulk form.

That the conductivity and switching which we observe during the course of the work is essentially ionic in character or not, the polarization experiments have been carried out and it has been found convincingly by blocking electrode measurements that it is the ionic migration which constitutes the major part of conductivity and is responsible for high conducting state i.e. switching effects are due to formation of interconnected phase between silver rich phase and silver deficient phase.

The present work explores the possibility of generalizing a high ionically conducting state in silica based glasses containing 10-30 mol %  $\text{Li}_2\text{O}$  and subjected to  $\text{Li}^+ \rightleftharpoons \text{Ag}^+$  ion exchange treatment.

---

## EXPERIMENTAL TECHNIQUES

The experimental set up involved in this present work from preparation of glasses of various compositions to characterisation techniques employed is our concern in this chapter.

## 2.1 PREPARATION OF GLASS :

The glasses of various compositions in the present studies are prepared with the conventional melting and annealing processes. The compositions investigated are given in the Table 3.1. The base material is  $\text{SiO}_2$  and  $\text{Li}_2\text{O}$ ,  $\text{B}_2\text{O}_3$ ,  $\text{CaO}$ ,  $\text{Al}_2\text{O}_3$ ,  $\text{Fe}_2\text{O}_3$  and  $\text{ZnO}$  are other oxides introduced.  $\text{Li}_2\text{O}$ ,  $\text{B}_2\text{O}_3$  and  $\text{CaO}$  are added as their respective carbonates.

All the starting materials such as  $\text{SiO}_2$ ,  $\text{Li}_2\text{O}$  etc. are mixed in appropriate proportions, and ground in pestle and mortar in a batch of 100 gms. each. The ground material is melted in alumina crucible using an electrically heated furnace at a temperature ranging between  $1000^\circ\text{C}$  -  $1200^\circ\text{C}$  for two hours. In the meantime it is stirred with a glass rod to make the melt homogeneous and bubble free. The melt is poured onto an aluminium mould and subsequently annealed at  $500^\circ\text{C}$  for four to five hrs. Now the glass is ready for sample preparation for various studies.

## 2.2 SAMPLE PREPARATION FOR ELECTRICAL CHARACTERIZATION:

For electrical measurements the glass pieces of the size of 10 mm x 10 mm x 2 mm and of dimensions of 2 mm x 2 mm x 2 mm for

ion-exchange purposes are cut and polished using the silicon carbide grit of different mesh sizes ( 100, 240, 320, 400, 600 and 800 respectively). The dimensions of the specimens are accurately measured by a micrometer ( MITUTOYA MAKE). Two opposite faces of the samples are electrode coated with silver paint ( NPL, India) and put in the conductivity cell for the resistivity versus temperature measurements. The conductivity cell consists of a stainless steel jacket within which is enclosed an electrode system. Two rectangular stainless steel plates, which act as electrodes by sandwiching the sample in between them, form the electrode system. The electrodes pass through the glass tubings which have spring arrangements so that electrodes can be moved up and down as per the dimensions of the sample. The lower electrode is supported on an alumina substrate which itself is attached rigidly to the main structure of the cell. The two electrodes are well shielded by metallic shielding. The central rod forms the spinal cord of the conductivity cell which imparts strength to the whole structure. Figure 2.1 is the schematic representation of the conductivity cell.

A chromel-alumel thermocouple is fitted near the rectangular plates to measure the temperature of the sample. The upper end of the jacket is closed with a teflon disc.

The whole assembly is put in a furnace which can go up to 500°C with an accuracy of  $\pm 1^\circ\text{C}$ . INDOTHERM-401 ( Indotherm Industries Pvt. Ltd.) temperature controlled has been used to control the temperature.

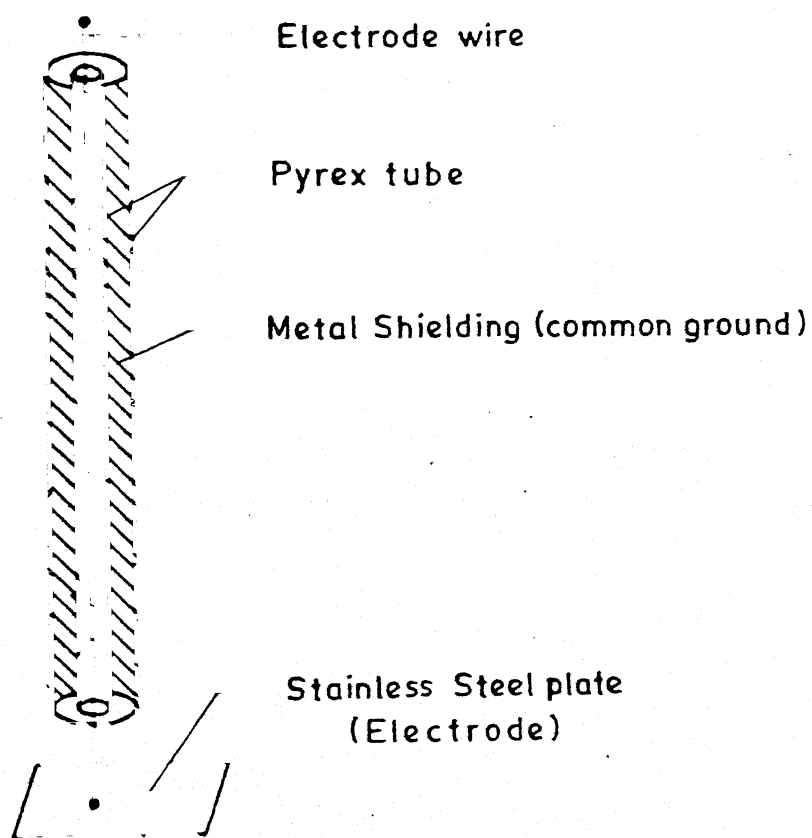
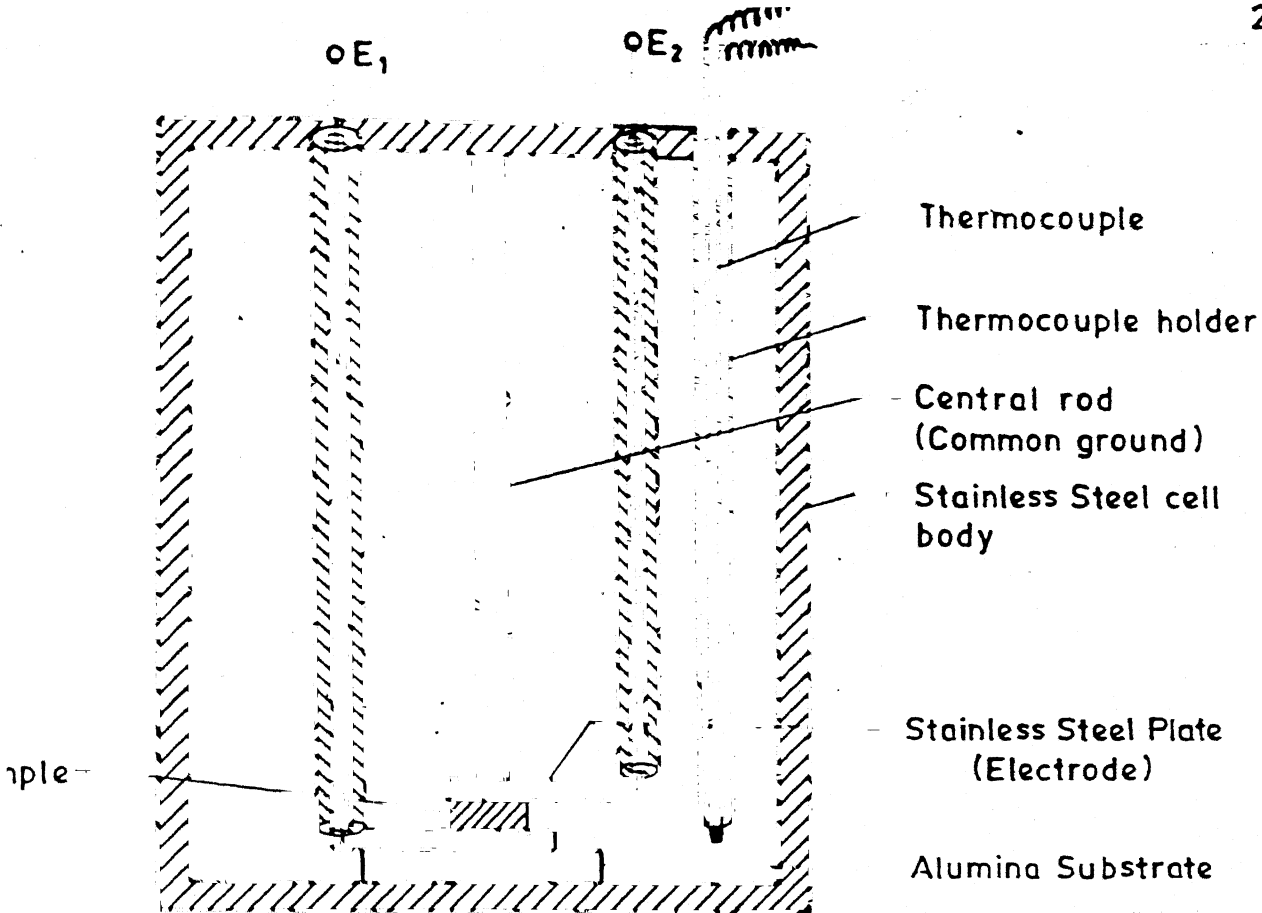


Fig. 2.1 Schematic view of the conductivity cell.

### 2.3 D.C. RESISTIVITY MEASUREMENTS :

Fig. 2.3 schematically represents the circuit diagram used for the measurements of I-V characteristics of different glass samples. The sample and the standard resistance are in series with a 30 volt 2 Amps. D.C. regulated power supply (APLAB MODEL 7152). The potential drop across the standard resistance is fed to the Y axis on XY recorder (No. 2000, made by Digital Electronics Ltd., India) and that across the sample to the X axis of the recorder. By changing the applied voltage by the power supply the I-V characteristics are automatically drawn on XY recorder of the sample.

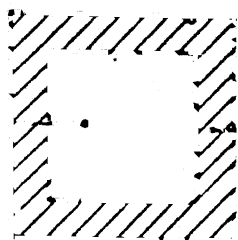
The I-V characteristics are drawn at temperatures from room temperature to 350°C with an interval of 25-30°C. Before making measurements the stability of the temperature is ensured.

Several I-V characteristics are drawn by changing the standard resistance at each temperature.

### 2.4 A.C. RESISTIVITY MEASUREMENTS :

A.C. measurements consist of measuring capacitance and dissipation factor at different frequencies for each temperature. The General Radio GR 1615 transformer ratio arm capacitance bridge with GR 13106 oscillator bench and GR 1232 tuned amplifier and a null detector are used to measure the capacitance and dissipation losses. The frequency range

Virgin Glass



Ion-exchanged  
(Silver-rich Layer)

Fig.2.2 Schematic representation of the morphology of ion-exchanged sample.

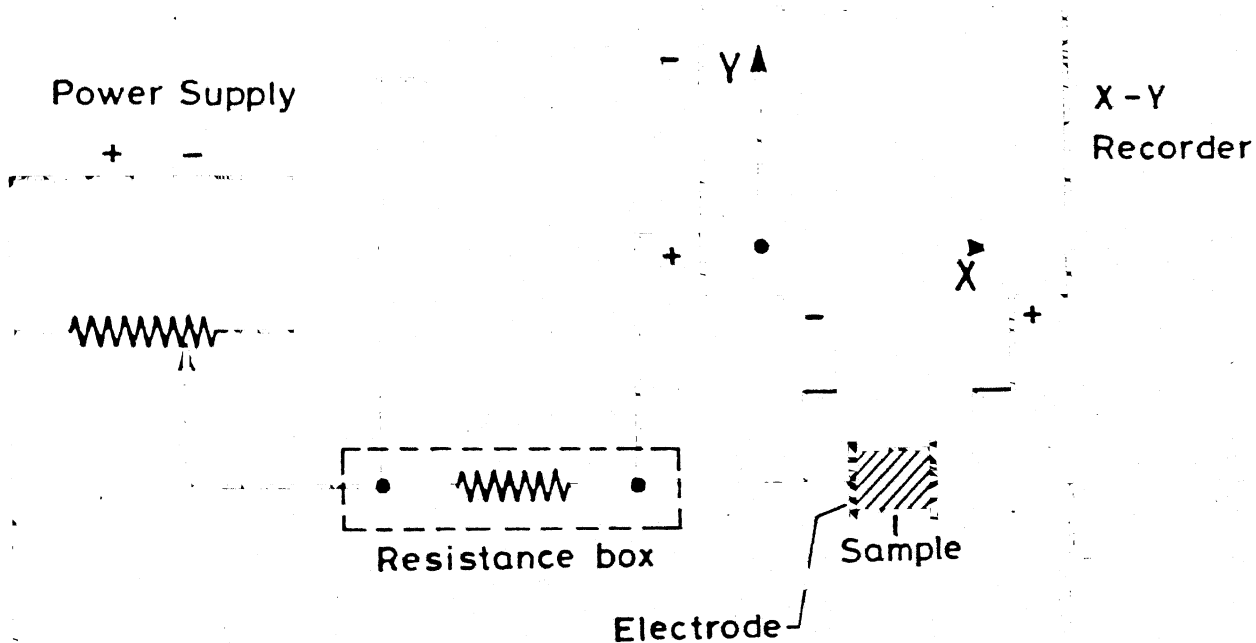


Fig.2.3 Schematic circuit diagram for DC Resistivity measurements.



is from 100 Hz to 100 kHz.

The resistance is calculated from the relation

$$\tan\delta = \frac{1}{\omega RC} \quad \dots \quad (2.1)$$

$$\text{Since } \frac{1}{R} = G$$

$$G = \omega C \tan\delta \quad \dots \quad (2.2)$$

where R is total Resistance, G is conductance and  $\tan\delta$  is dissipation factor and C is capacitance at the frequency  $\omega$ .

The complex impedance can be shown to be

$$Z = Z' - iZ'' \Rightarrow \frac{G}{G^2 + \omega^2 C^2} - i \frac{\omega C}{G^2 + \omega^2 C^2} \quad (2.3)$$

Here we see -

$$Z' = \frac{G}{G^2 + \omega^2 C^2} \quad \dots \quad (2.4)$$

and

$$Z'' = \frac{\omega C}{G^2 + \omega^2 C^2} \quad \dots \quad (2.5)$$

If we eliminate  $\omega$  between equations (2.4 and 2.5) we obtain the expression:

$$Z'^2 + Z''^2 - \frac{1}{G} Z' = 0 \quad \dots \quad (2.6)$$

which is the equation of circle with centre  $(\frac{1}{2G}, 0)$  and radius  $\frac{1}{2G}$ .

So by knowing the radius of the circle we obtain the value of d.c. conductance/resistance of the sample and that value is converted into resistivity by modifying with the sample dimensions.

$$\rho_{dc} = \frac{A}{t} R_{dc} \quad \dots \quad (2.7)$$

where A is the area of cross section and t is the thickness of the sample.

The  $\log \rho$  vs.  $\frac{1}{T}$  curve is plotted and activation energy value Q is calculated by using the well known relation:

$$\rho = \rho_0 \exp \frac{Q}{kT} \quad \dots \quad (2.8)$$

where Q is activation energy,  $\rho_0$  is the pre-exponential factor, k is the Boltzmann's constant, and T is the absolute temperature.

## 2.5 SAMPLE PREPARATION FOR ION EXCHANGE :

Well polished and cleaned samples of the dimension of about 2 mm x 2mm x 2 mm, are kept in a pyrex boat containing molten silver nitrate at 330°C for 48 hours in an electrically heated furnace. After the ion exchange the glass samples are washed thoroughly and boiled in water for 2-3 hours to ensure the elimination of any silver nitrate sticking onto the sample surfaces. Finally samples are washed in acetone, dried and kept in a desiccator. Fig 2.2 shows schematically the ion exchanged portion of a glass sample.

The electrical resistivity measurements for ion exchanged samples are done exactly in the same manner as for the virgin

glasses discussed in section 2.3 and section 2.4.

## 2.6 X- RAY ANALYSIS :

The x-ray diffractograms for the various glass systems in the virgin, ion-exchanged and switched state, respectively, have been taken after thoroughly grinding them in an agate mortar to a very fine particle size ( $\sim 10 \mu\text{m}$ ). 'Rich Seifert 2002D Isodebye Flex diffractometer' with  $\text{CuK}\alpha$  radiation ( wave length  $1.542 \text{ \AA}$ ) has been used to record the x-ray diffraction pattern of the glass systems at a scanning speed of  $3^\circ$  per minute with counter position ( $2\theta$ ) from  $5^\circ$  to  $90^\circ$ .

## 2.7 DIFFERENTIAL THERMAL ANALYSIS :

The knowledge of glass transition temperature is very important for us,, since all ion exchange is done well below this temperature. Differential thermal analysis is a reliable and useful technique for this purpose. It consists of measuring temperature differences between a sample and a standard material as both are heated or cooled at a constant rate. The temperature difference between the two is measured by a thermocouple in the form of EMF. The standard sample is so chosen that (i) it does not undergo phase transitions in the temperature range of interest so that there is no ambiguity of the origin of the observed heat effects (ii) it has nearly the same heat capacity as the sample, thus minimising the drift of the differential EMF and (iii) it has nearly the same density as the sample, in order that volumes of the sample and standard specimen are comparable.

In the present studies Alumina  $\text{Al}_2\text{O}_3$  has been chosen as the standard material.

When neither the sample nor standard specimen undergo a phase transition both will be at the same temperature and there will be no signal from the differential thermocouple. If however, sample undergo a phase transition heat will be absorbed or released as per the transition is endothermic or exothermic. This will result in decrease or increase of the temperature of the sample respectively and will be recorded by differential thermocouple.

When the glass transition takes place, heat is absorbed which causes the temperature of the glass sample to decrease as compared to the standard specimen  $\text{Al}_2\text{O}_3$ . The differential EMF is recorded by DTA processor directly in terms of temperature difference on a curve  $\Delta T$  vs.  $T$ .

where  $\Delta T$  is the difference in the temperature corresponding to differential thermal EMF.

## 2.8 BLOCKING ELECTRODE MEASUREMENTS :

Wagner's (1955) asymmetric polarization cell technique has been used to distinguish between the ionic and electronic conductivity type. The silver paint (NPL, India) on one face of the sample serves as the reversible electrode and replenishes the silver ions whereas the graphite paint (Polaron Equipment Ltd., England) acts as the blocking electrode on the other phase of the sample.

The cell Ag/High conducting glass system/ $C^+$  is clamped in the sample holder. A small polarising voltage of the order of 100 mV is applied to the sample in series with a standard resistance. The current in the circuit is measured as a function of time. As the time lapses the resistance of the sample goes on increasing due to polarization of the sample resulting in continuous increase of voltage drop across the sample. Therefore current in the circuit decreases with time. This variation is recorded by XY recorder. (Fig. 2.3).

--

## CHAPTER 3

## RESULTS AND DISCUSSION

The various compositions investigated in the present work are given in Table 3.1. The results obtained on investigation of these compositions using various techniques such as electrical, X-ray Diffraction Analysis, DTA, Density Measurements respectively form the subject of this chapter.. Various results for virgin ( without ion exchange) and ion exchanged glasses ( both before and after switching) have been discussed in keeping with the previous studies carried out on silicate glasses. The virgin glass systems are referred to as G1,G2 etc. The ion-exchanged glass systems before switching are referred to as IG1, IG2 etc. and the high conducting glass systems after switching are referred to as HIG1, HIG2 etc. as per the compositions given in the Table 3.1.

## 3.1 X-RAY ANALYSIS:

The X-ray diffractograms for the various glass systems have been taken in the virgin, ion-exchanged and switched states respectively with counter position ( $2\theta$ ) from  $5^\circ$  to  $90^\circ$  and at scanning speed  $3^\circ$  per minute.

A broad peak is observed which indicates that all of them are amorphous.

Figure 3.1 to Figure 3.3 show the x-ray diffraction pattern for the glass systems G1,G2 and HIG2 respectively.

TABLE 3.1 Composition of glass systems

Sl. No.	Glass system no.	Mole %						
		Li <sub>2</sub> O	CaO	Al <sub>2</sub> O <sub>3</sub>	B <sub>2</sub> O <sub>3</sub> *	ZnO	Fe <sub>2</sub> O <sub>3</sub>	SiO <sub>2</sub>
1	G1	20	13	3	4	-	-	60
2	G2	30	-	-	-	12	-	58
3	G3	30	12	3	-	-	-	55
4	G4	10	13	3	10	-	-	64
5	G5	30	-	-	-	9	3	58

TABLE 3.2 DENSITY AND GLASS TRANSITION TEMPERATURES

Sl. No.	Glass system no.	Density (specific gravity)	Glass transition Temperature (°C)
1	G1	2.882	420
2	G2	2.961	475
3	G3	2.8447	510
4	G4	2.7145	460
5	G5	2.916	380

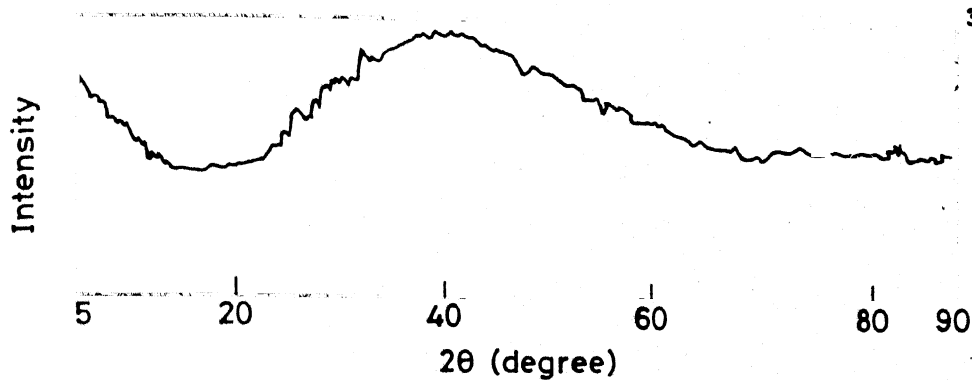


Fig. 3.1 X-ray diffraction pattern for glass system G1.

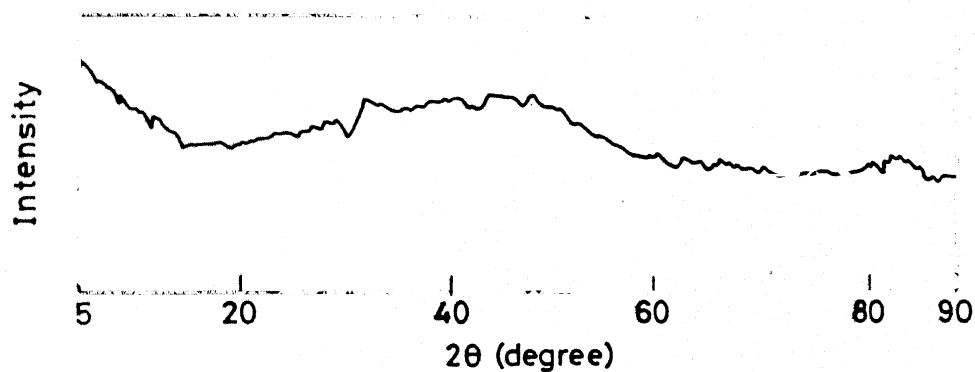


Fig. 3.2 X-ray diffraction pattern for glass system G2.

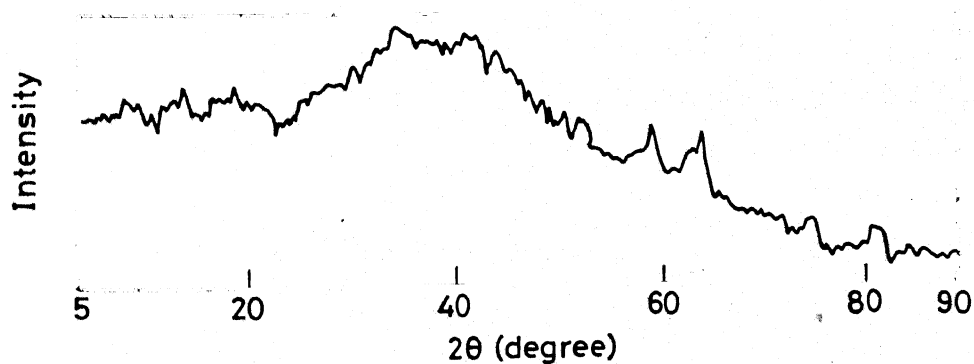


Fig. 3.3 X-ray diffraction pattern for glass system (high conducting state) HIG 2.



### 3.2 DIFFERENTIAL THERMAL ANALYSIS :

The Differential Thermal Analysis has been done for all compositions to find the transition temperatures of the glass samples. The knowledge of transition temperature is essential because the ion-exchange is done well below the glass transition temperature to ensure that no permanent structural changes take place in the glass network and it is only this temperature upto which all our measurements are carried out. The Table 3.2 shows the transition temperature for various glass systems...

Figure 3.4 to Figure 3.6 represent the glass transition temperatures for the glass systems G1, G3 and G5 respectively.

### 3.3 DENSITY MEASUREMENTS :

The specific gravity measurements have been made using simple Archimedes principle. Benzene ( Specific Gravity 0.8) has been used as the liquid for the measurements. Water is not used as lithium-silicate glasses are hygroscopic.

Table 3.2 shows density (specific gravity) and glass transition temperatures for various glass compositions.

### 3.4 ELECTRICAL MEASUREMENTS :

The AC electrical measurements for the glass systems have been carried out as discussed earlier in Section 2.4 and D.C. electrical measurements have been made by XY recorder as described in Section 2.3 and circuit diagram as shown in Fig. 2.3.

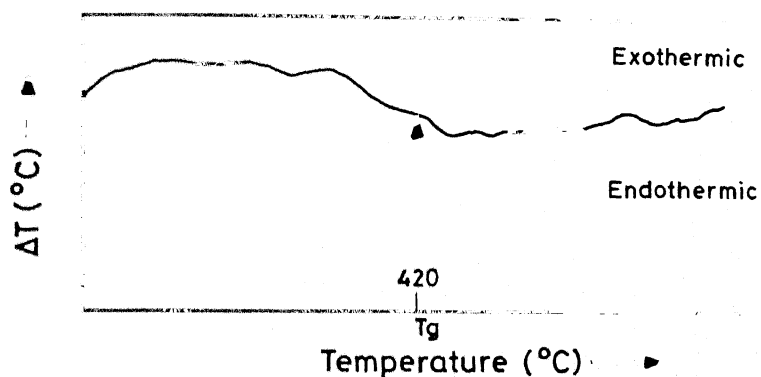


Fig. 3.4 Differential thermal analysis curve for glass system G1.

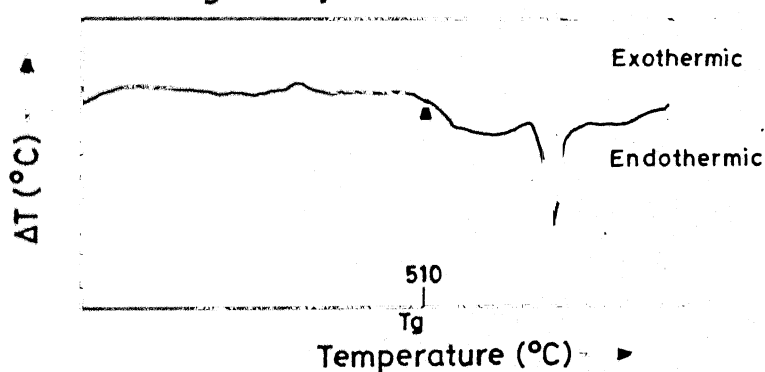


Fig. 3.5 Differential thermal analysis curve for glass system G3.

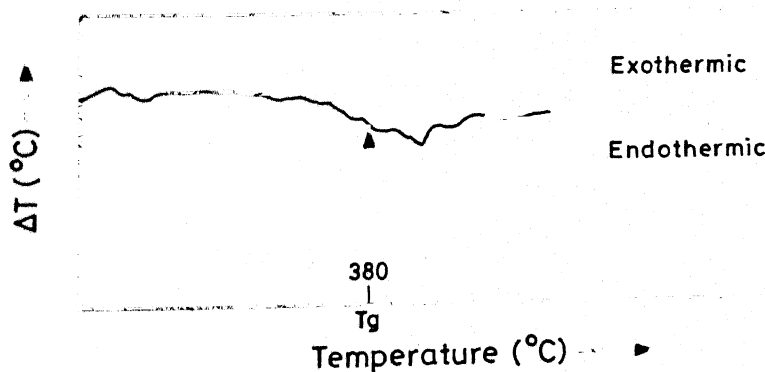


Fig. 3.6 Differential thermal analysis curve for glass system G5.

### 3.41 A.C. MEASUREMENTS:

The glass sample is made an arm of a simple Wheatstone (a.c.) bridge. A position of minimum deflection is obtained on the detector and the corresponding values of capacitance  $C$  and dissipation factor  $D (= \tan \delta)$  are noted at different frequencies ranging from 100 Hz to 100 KHz. The impedance analysis carried out in section 2.4 shows that the real part ( $Z'$ ) equ. 2.4 and imaginary part ( $Z''$ ) equ. 2.5 of the impedance fit an equation of a circle (equ. 2.6) if we eliminate  $\omega$  from the  $Z'$  and  $Z''$  with the centre ( $R_{dc}/2, 0$ ) lying on the  $Z'$  axis. The resistance ( $R_{dc}$ ) value is obtained where the semicircle intersects the  $Z'$  axis. The points obtained have actually been found to lie on a semicircle.

The Figure 3.7 to Figure 3.11 represent the complex impedance plots ( $Z''$  versus  $Z'$ ) for various glass systems. The  $R_{dc}$  values have also been measured by an electrometer (610C Electrometer, Keithley Instruments) and it has been found that the resistance values measured by the A.C. bridge and by the electrometer are in satisfactory agreement and lie within 1-2% difference with each other. This lends reliability to our results.  $R_{dc}$  values are found with ac measurements upto a temperature range above which the bridge ceases to balance and resistivity is so low that dissipation losses are quite high and exceeds the limit of the bridge which is unity.

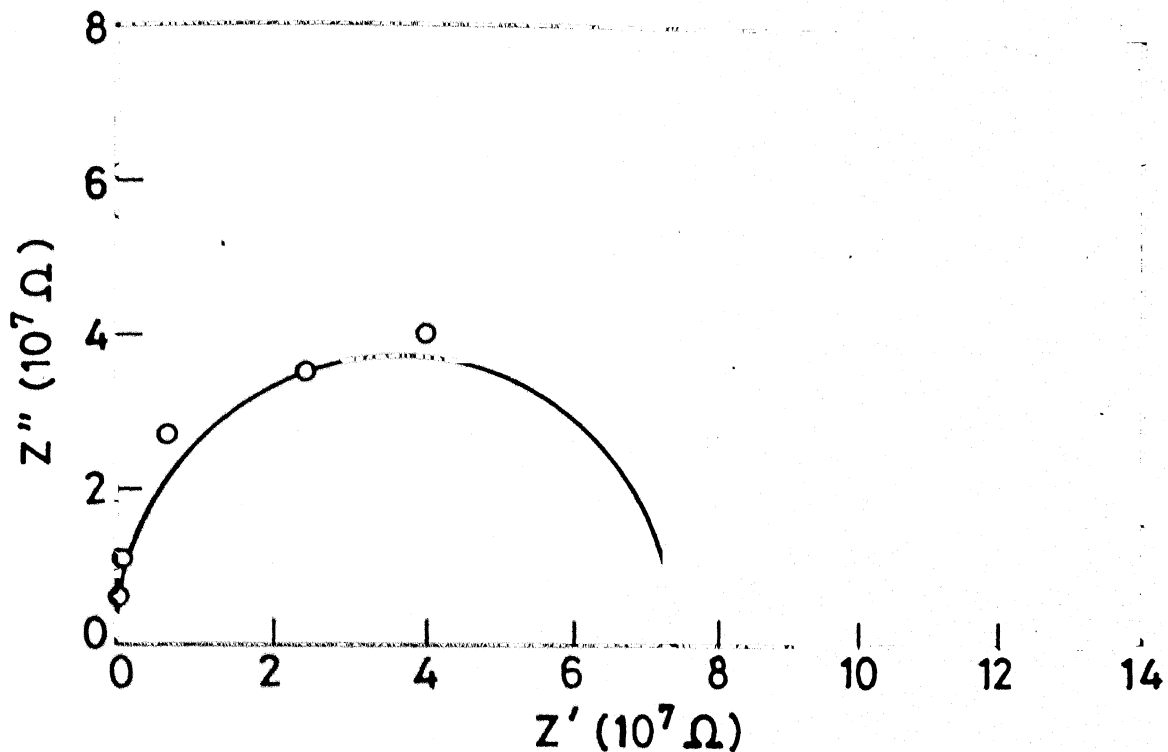


Fig. 3.7 Complex impedance plot for glass system G 1 ( $T = 66^\circ\text{C}$ ).

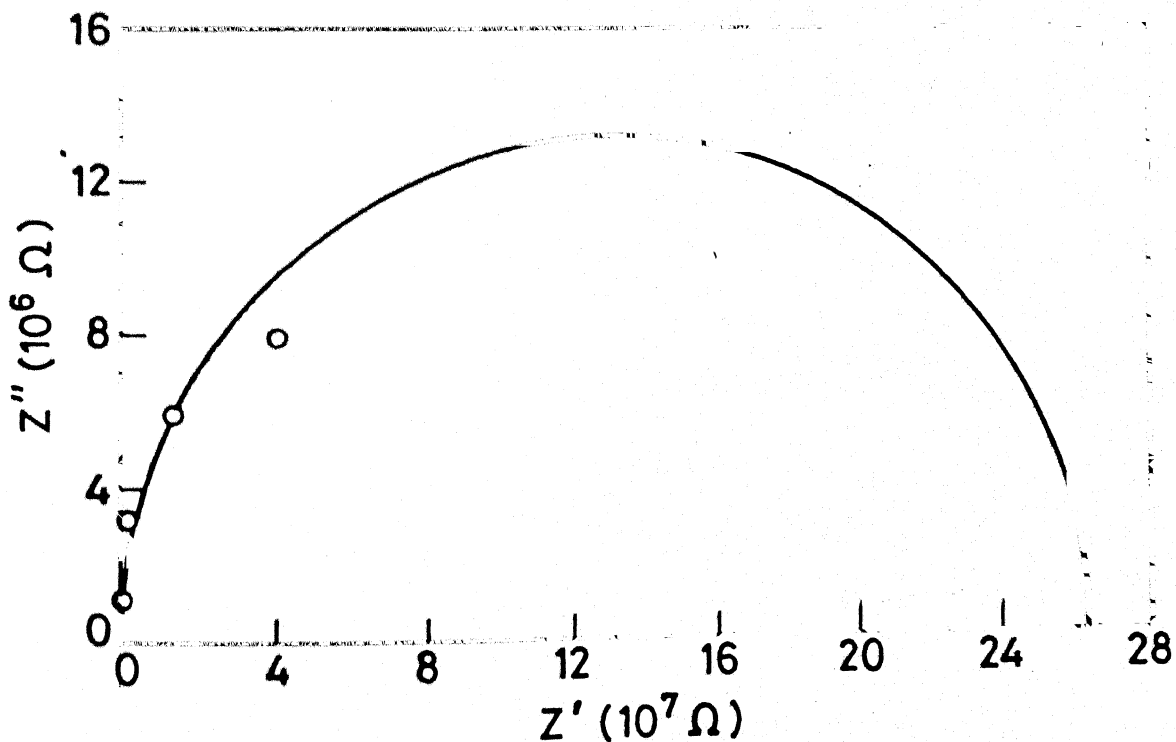


Fig. 3.8 Complex impedance plot for ion exchanged glass system IG 2 ( $T = 89.5^\circ\text{C}$ )

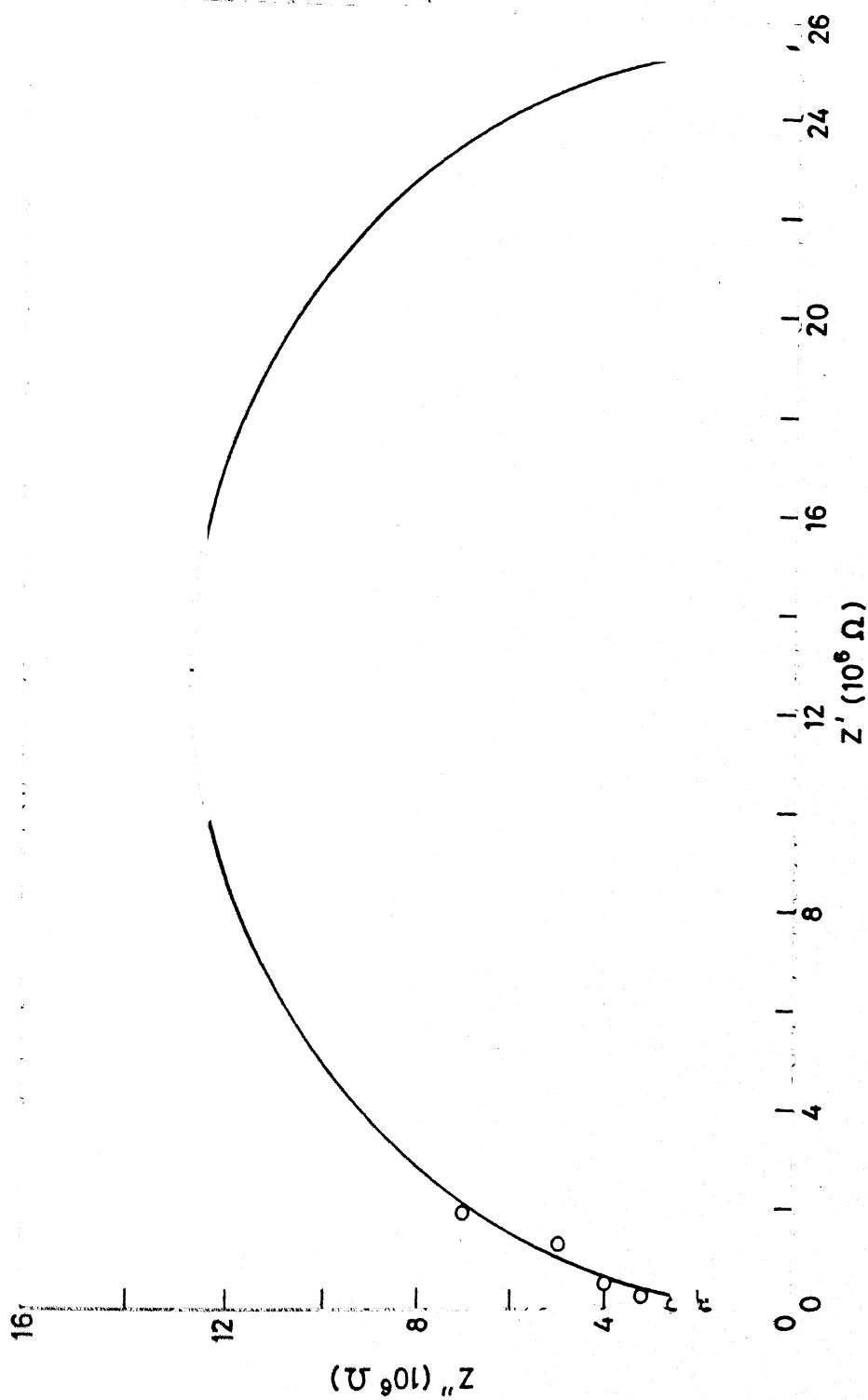


Fig. 3.9 Complex impedance plot for ion exchanged glass system IG1 ( $T = 114^{\circ}\text{C}$ )

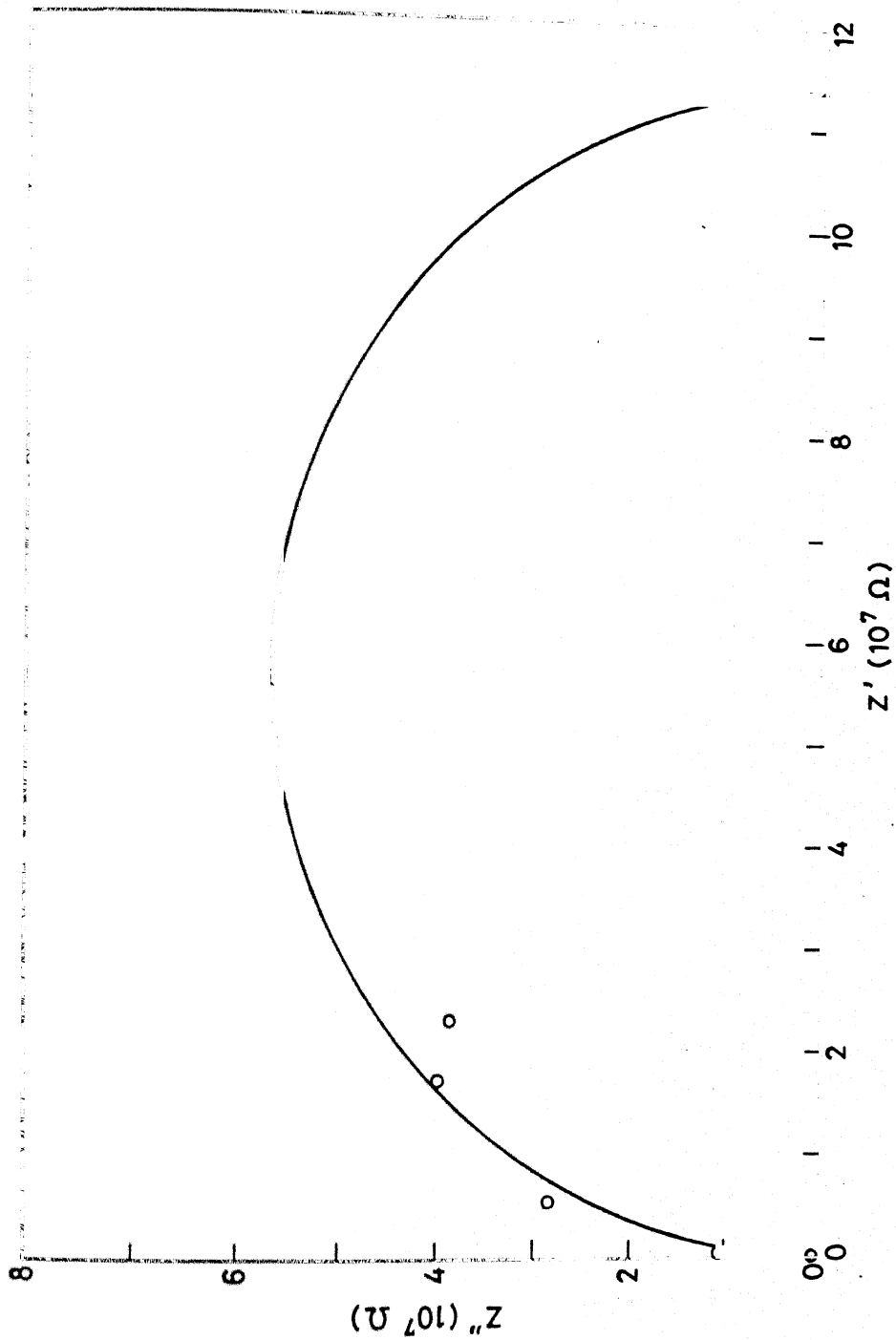


Fig. 3.10 Complex impedance plot for glass system G2 ( $T = 114.5^\circ\text{C}$ )

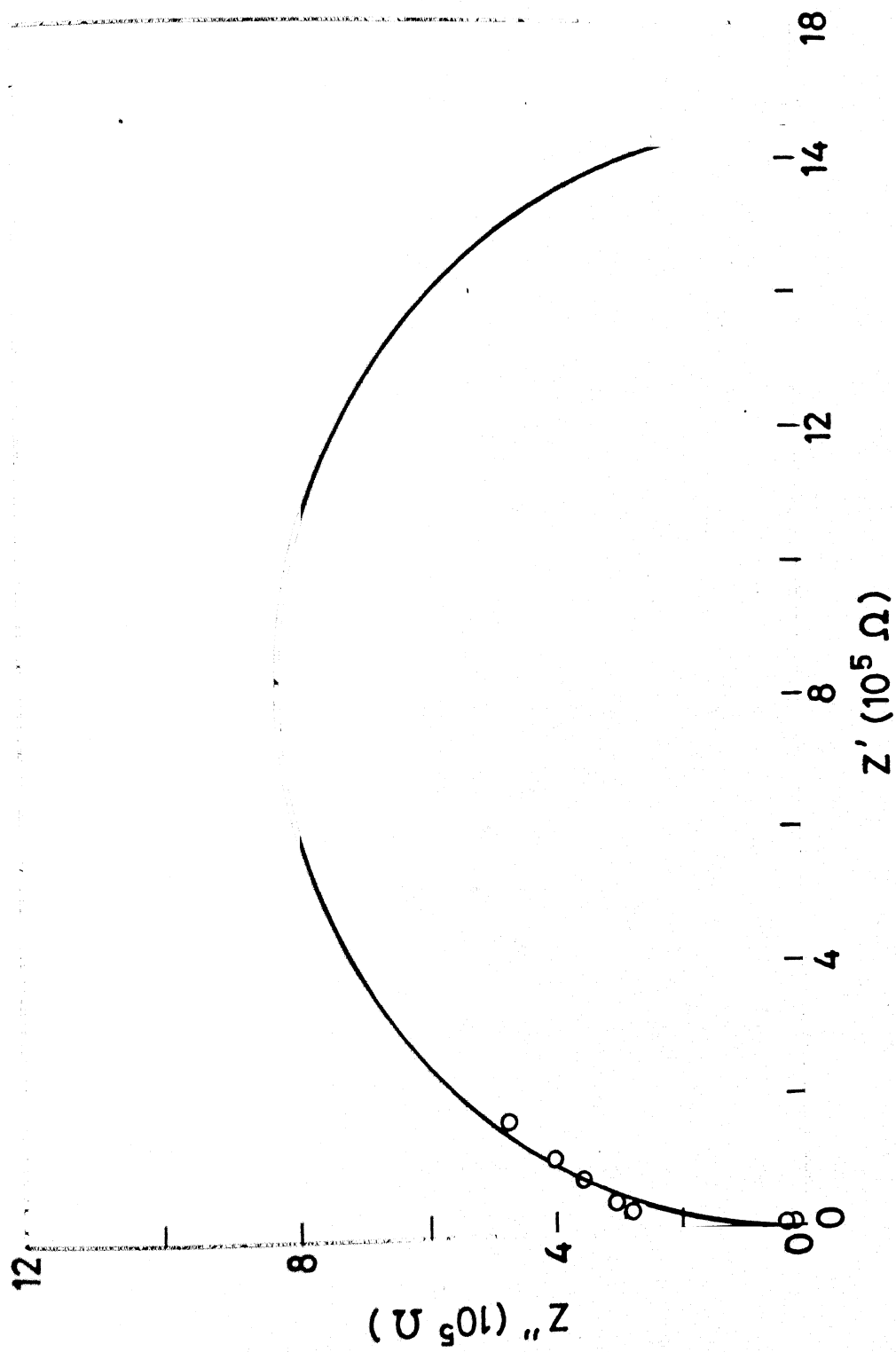


Fig. 3.11 Complex impedance plot for glass system G3 ( $T = 154.5^\circ\text{C}$ )

### 3.4.2 D.C. MEASUREMENTS :

I-V plots for the glass systems are obtained by XY recorder and dc resistances are obtained from the slopes of these curves. At a particular temperature two-three slopes are obtained by changing the standard resistance in series with the sample and the power supply and final value is obtained with different slopes to make the readings more reliable.

The resistance is converted into resistivity by multiplying it by factor  $\left( \frac{A}{t} \right)$ , where A is the cross sectional area of the sample and t is the thickness.

The measurements are made with an interval of 25-30°C from room temperature to around 350°C.

The temperature dependence of resistivity in each case being assumed to follow the relationship.

$$\rho = \rho_0 \exp \left( \frac{Q}{kT} \right) \quad \dots \quad (3.1)$$

where  $\rho$  = resistivity of the sample

$\rho_0$  = Pre-exponential factor

Q = Activation energy for conduction

K = Boltzman constant and T - Temperature in Kelvin.

The  $\ln \rho$  vs  $\frac{1}{T}$  curves have been found to be straight lines in each case except composition no. 2 in which a kink is obtained in virgin glass system G and glass system IG (ion exchanged before switching).



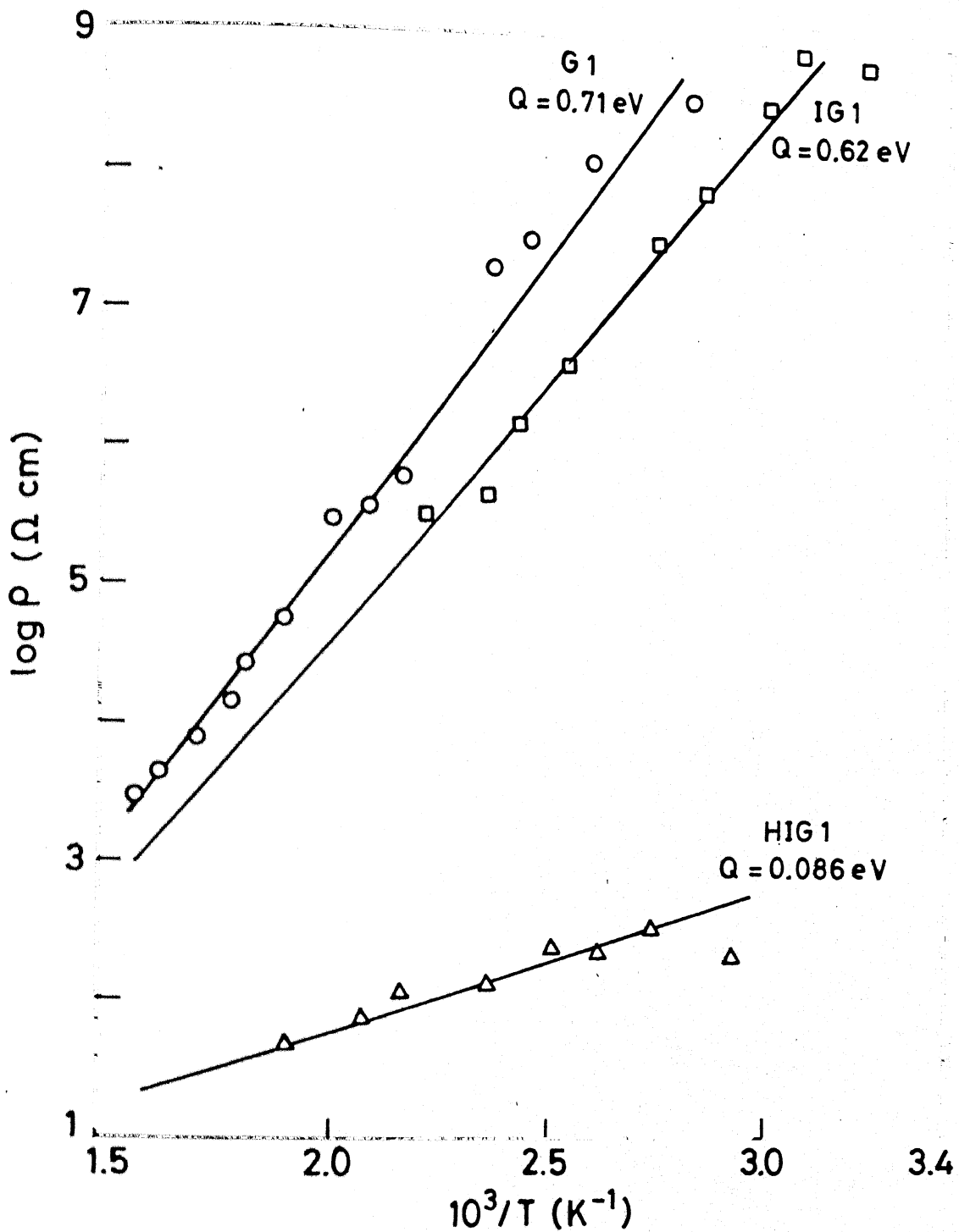


Fig. 3.12 Temperature variation of DC resistivity for glass systems G1, IG1, and HIG1.

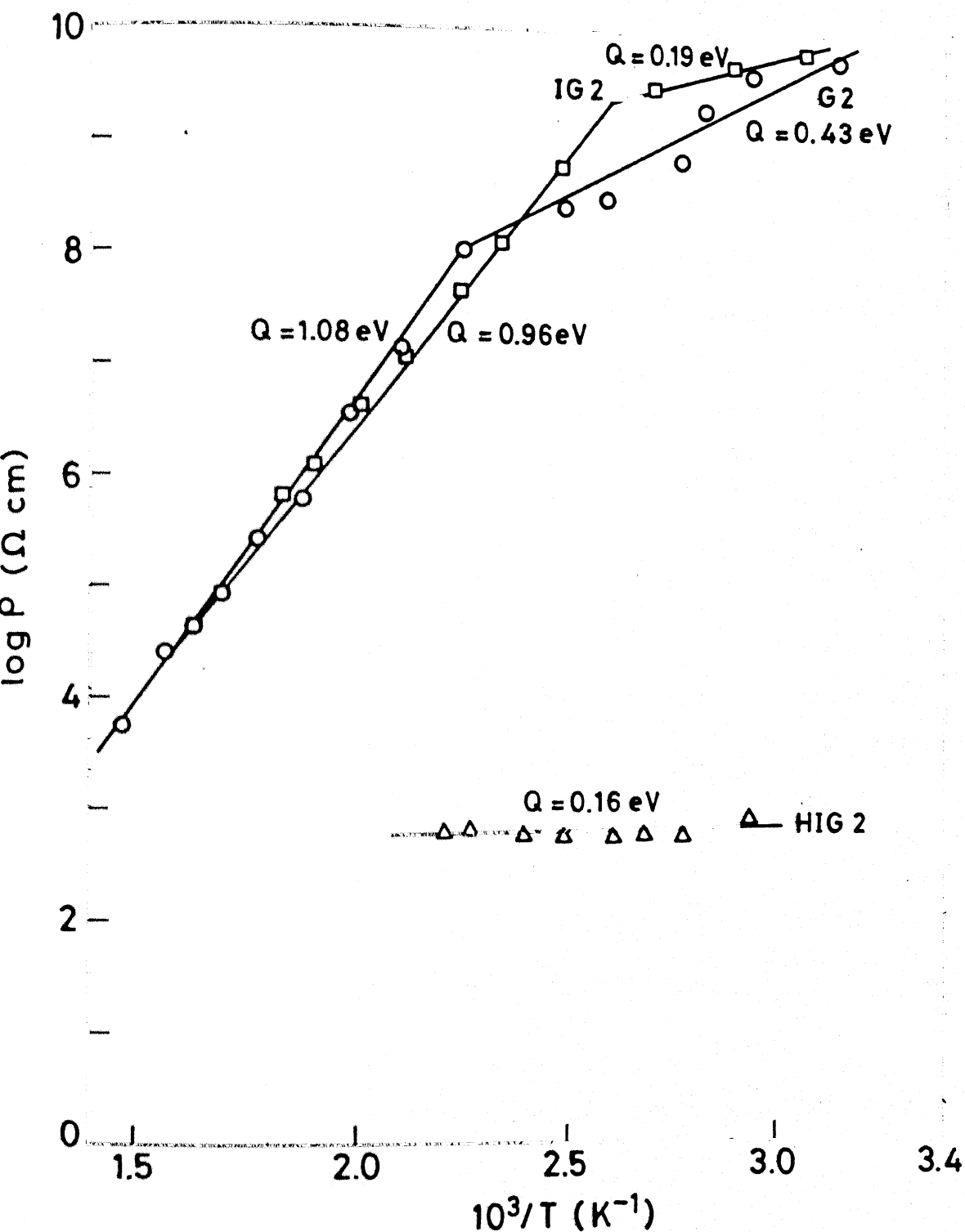


Fig. 3.13 Temperature variation of DC resistivity for glass systems G2, IG 2 and HIG 2.

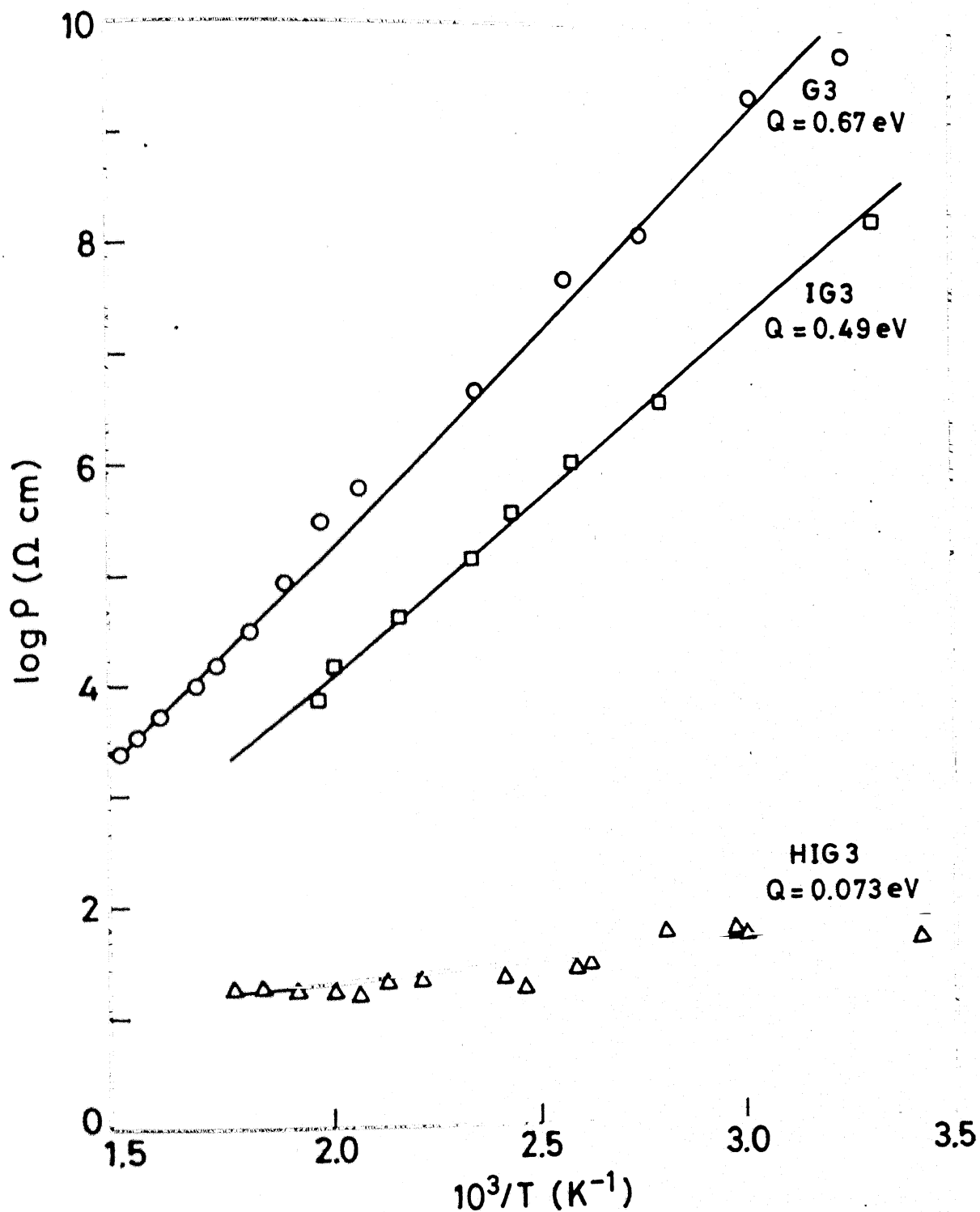


Fig. 3.14 Temperature variation of DC resistivity for glass systems G3, IG3 and HIG3.

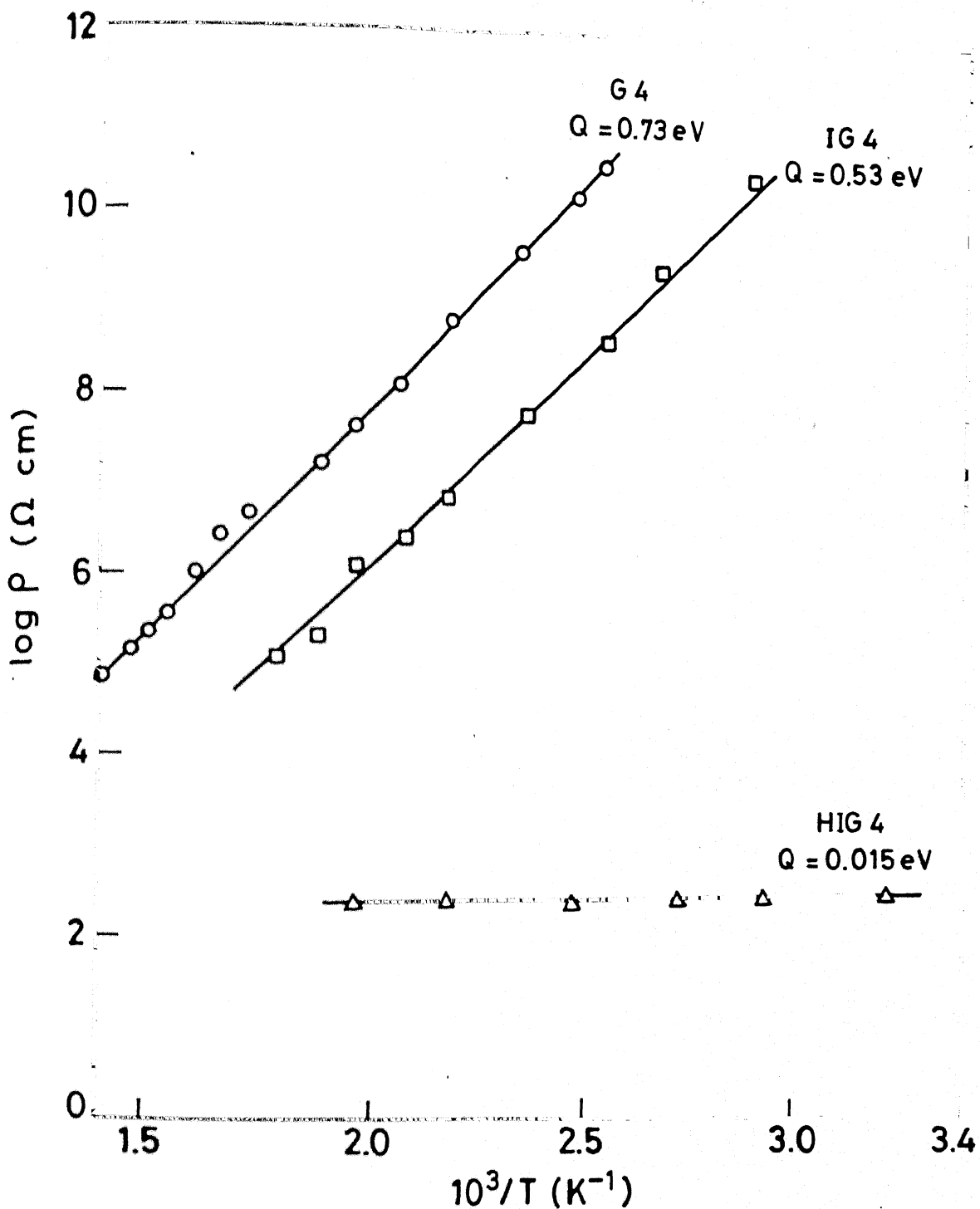


Fig. 3.15 Temperature variation of DC resistivity for glass systems G4, IG 4 and HIG 4.

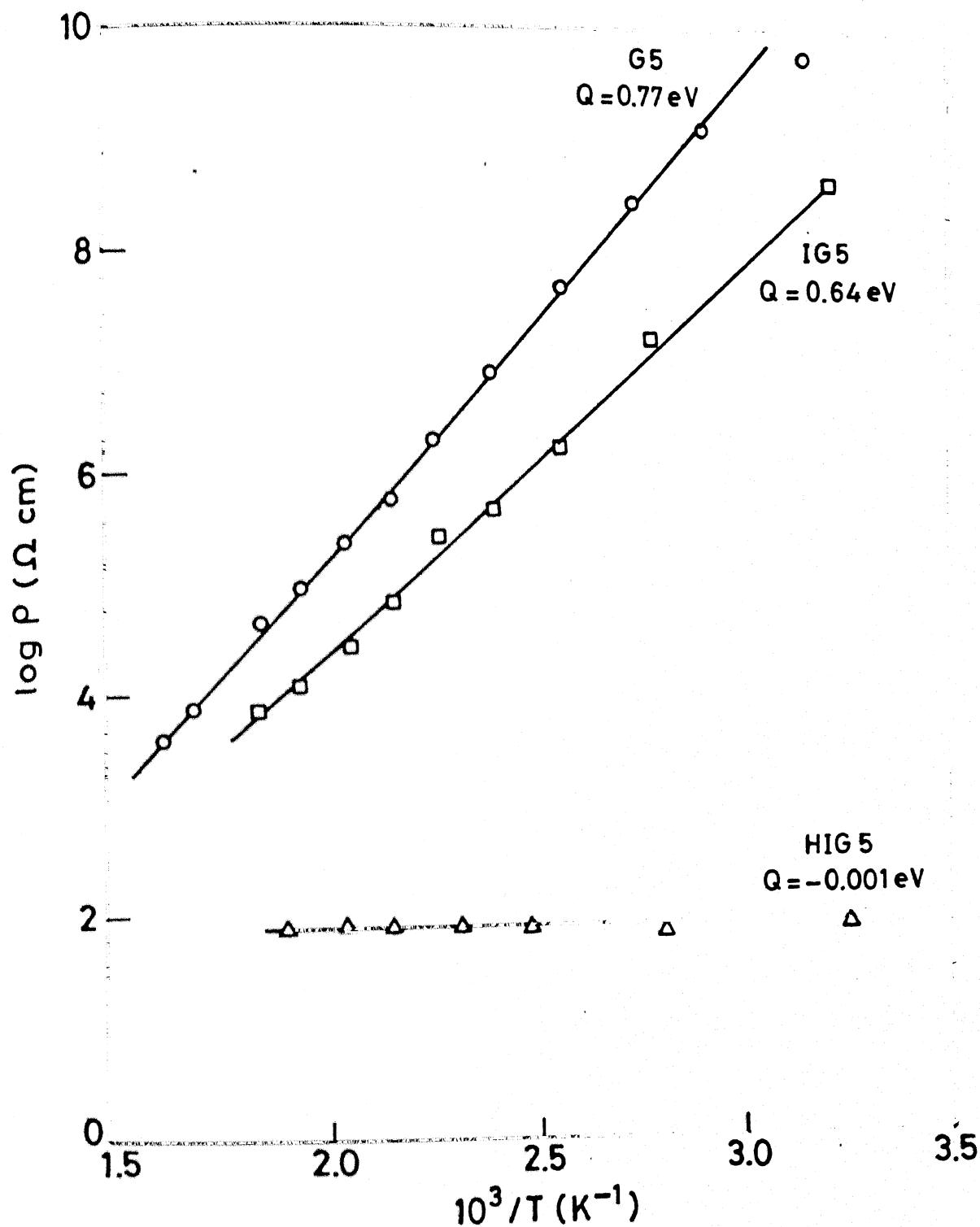


Fig. 3.16 Temperature variation of DC resistivity for glass systems G5, IG5 and HIG5.

The ion exchanged glass systems of all compositions switch to a high conducting state when we use a particular amount of field at a particular temperature. This high conducting state is quenched by applying same temperature and field at which it switches. It is seen this state is stable upto about the temperature of switching.

Fig. 3.12-3.16 show the plots of  $\log \rho$  Vs  $1/T$  for virgin G, ion-exchanged (IG) and high conducting (HIG) glass systems.

Tables 3.3 to 3.7 list the values of pre-exponential factor  $\rho_0$  and the activation energy  $\Omega$  for each composition separately for virgin (G), ion exchanged before switching (IG) and Ion-exchanged after switching (HIG) states.

Figures 3.17 to Figure 3.21 typify the switching phenomena observed for each composition respectively.

### 3.4.3 : DISCUSSION :

The observed low activation energy and resistivity values as the lithium content increases arise because of the lower activation barrier to ionic transport. It has been shown (Stevens 1957) that the activation barrier to the ionic transport in oxide glasses consists of two components viz., electrostatic and mechanical. The increasing amount of  $\text{Li}_2\text{O}$  results in an enhancement of nonbridging oxygen ions and thereby causing more openness of the network (Rawson 1984) and if the glass network is sufficiently open which is the case when enough ions are present (valid in our glass systems), contribution due to the elastic distortion

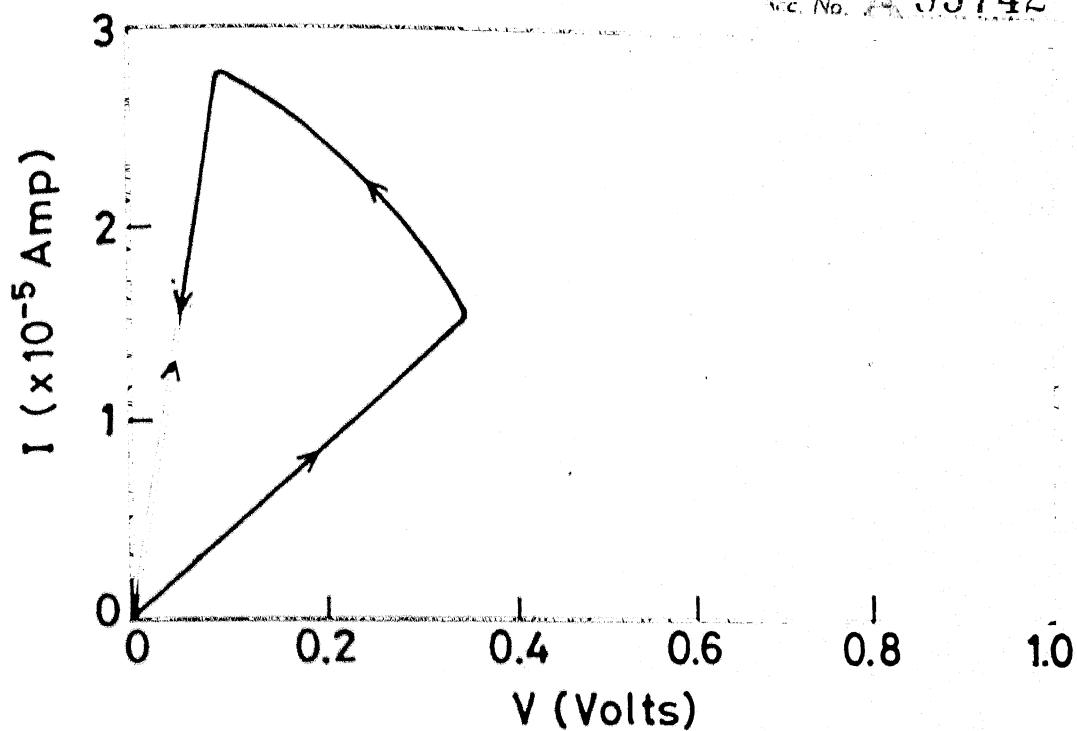


Fig. 3.17 Switching of glass system IG3 ionexchanged at  $330^{\circ}\text{C}$  to HIG 3 state ( $T_c=285^{\circ}\text{C}$ ).

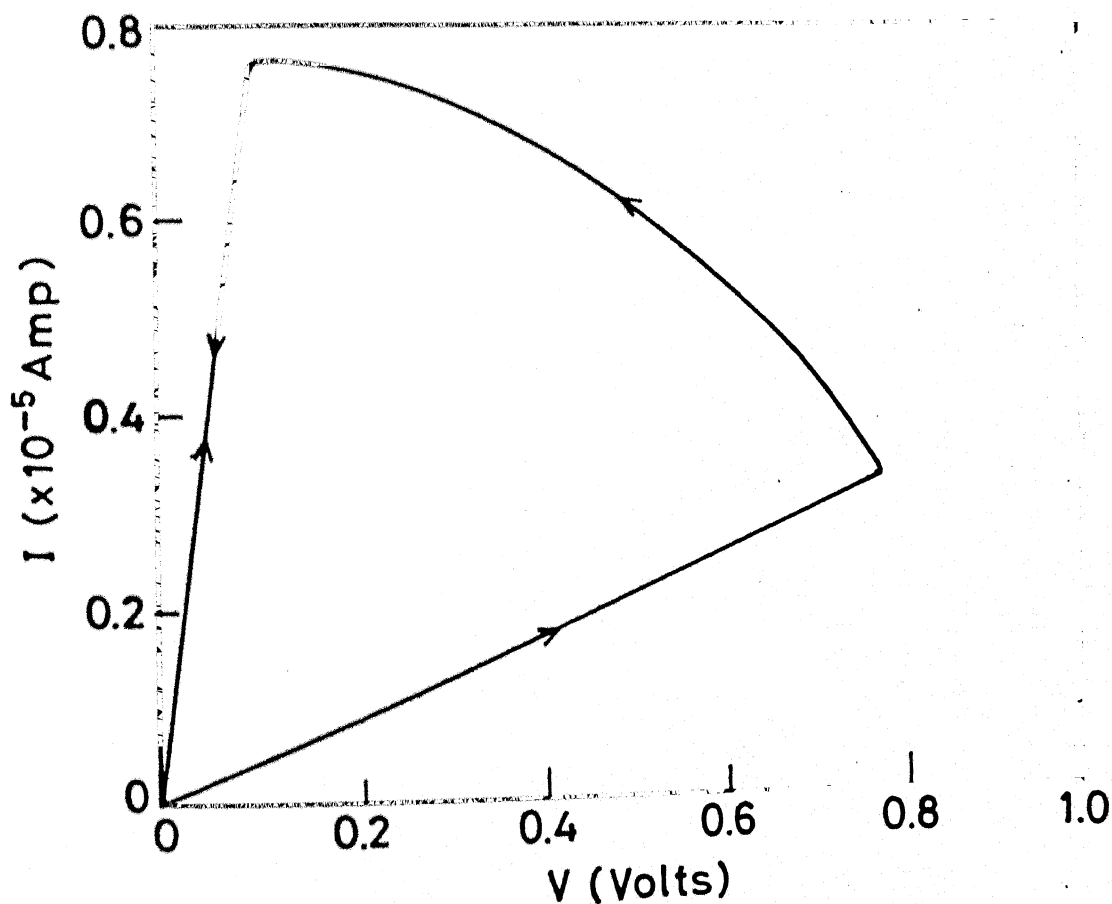


Fig. 3.18 Switching of glass system IG1 ionexchanged at  $330^{\circ}\text{C}$  to HIG 1 state ( $T_c=181.5^{\circ}\text{C}$ ).

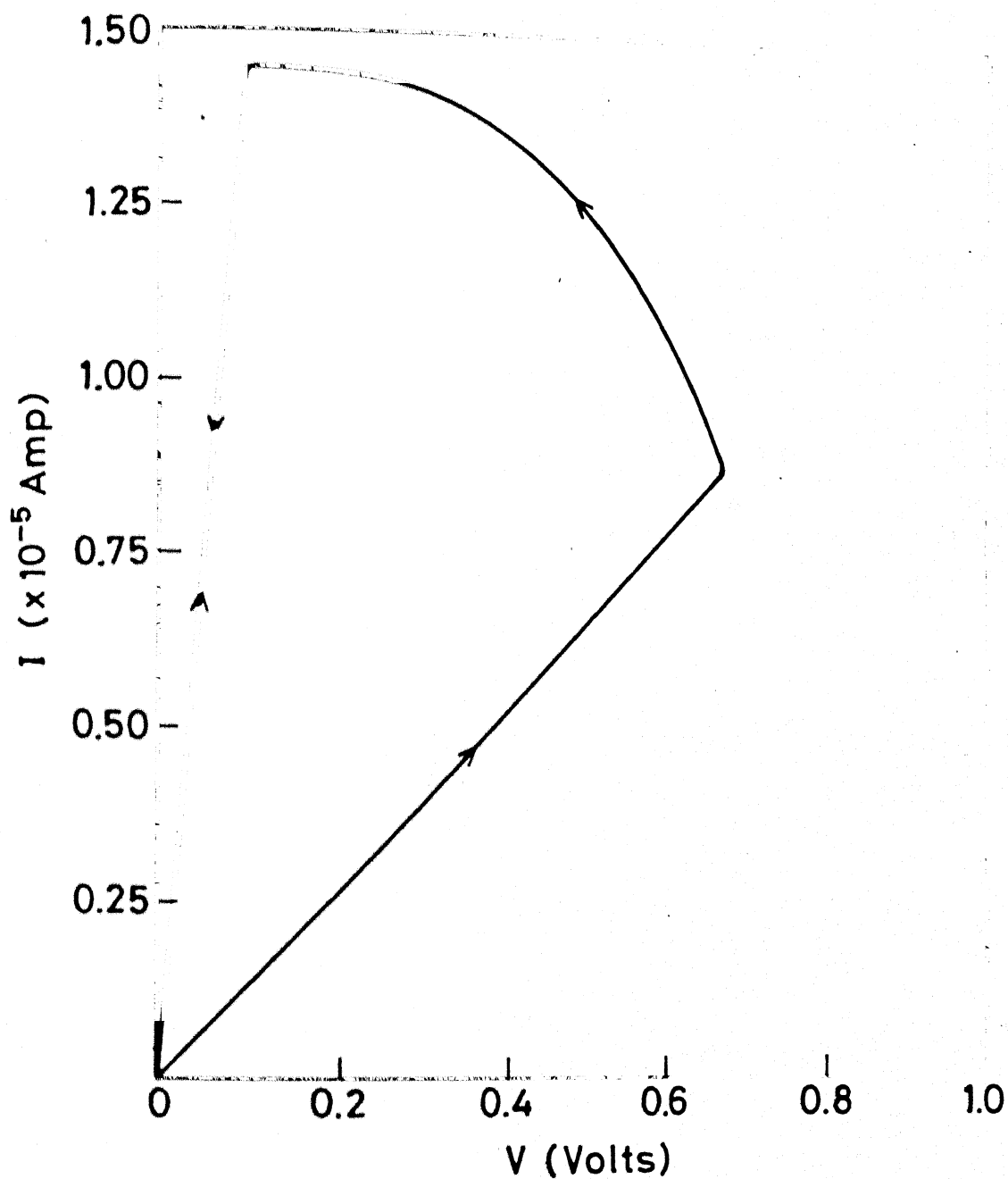


Fig.3.19 Switching of glass system IG 2 ionexchanged at 330°C to high conducting state HIG 2 ( $T_c=318.5^\circ\text{C}$ )



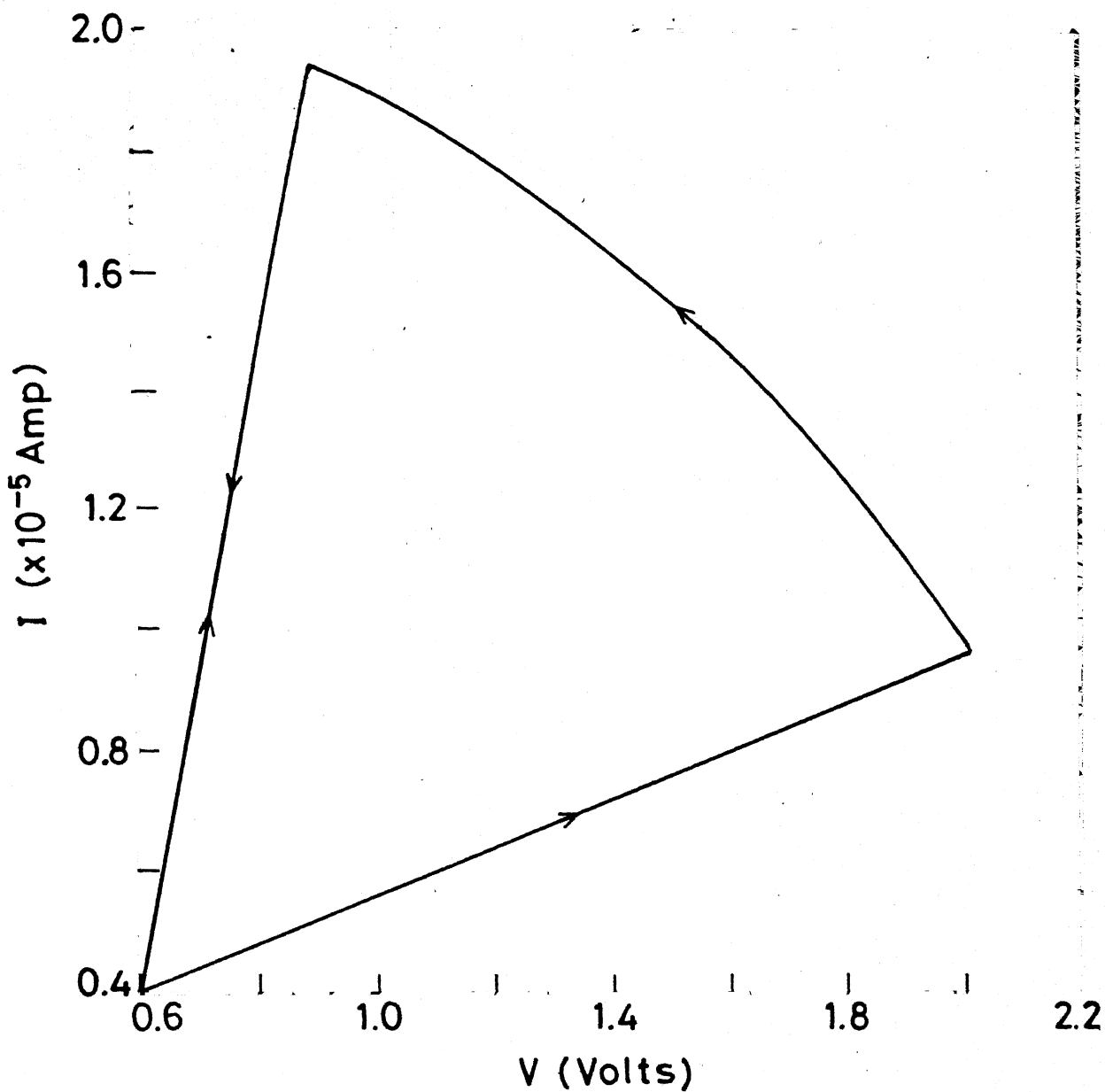


Fig. 3.20 Switching of glass system IG4 ionexchanged at  $330^{\circ}\text{C}$  to high conducting state HIG 4 ( $T_c=259.5^{\circ}\text{C}$ ).

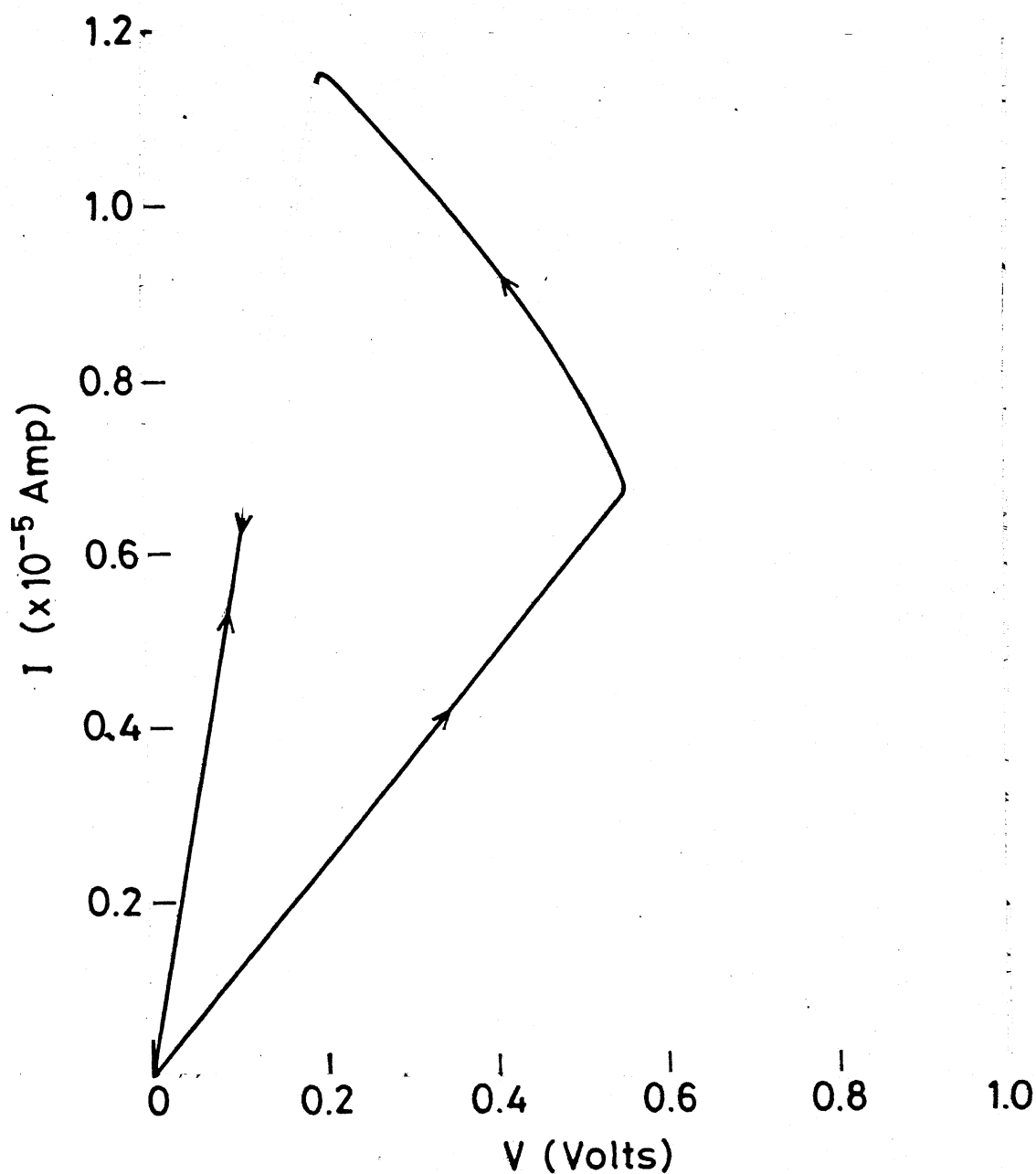


Fig. 3.21 Switching of glass system IG5 ionexchanged at 330°C to high conducting state HIG5 ( $T_c=273^\circ\text{C}$ ).

TABLE 3.3 Activation energy ( $Q$ ) and pre-exponential ( $\rho_0$ ) factors for glass composition no. 1

Sl. no.	Glass system	$Q \pm \Delta Q$ (eV)	$\rho_0$ (ohm cm)
1	G1	$0.71 \pm 0.20$	$1.2 \times 10^{-2}$
2	IG1	$0.62 \pm 0.23$	$5.3 \times 10^{-2}$
3	HIG1	$0.01 \pm 0.01$	10.62

TABLE 3.4 Activation energy( $Q$ ) and pre-exponential ( $\rho_0$ ) factors for glass composition no. 2

Sl. No.	Glass system	$Q \pm \Delta Q$ (eV)	$\rho_0$ (Ohm cm)
1	G2	$1.08 \pm 0.13 / 0.43 \pm 0.21$	$7.03 \times 10^{-3}$
2	IG2	$0.96 \pm 0.24 / 0.19 \pm 0.15$	$5.5 \times 10^{-4}$
3	HIG2	$0.16 \pm 0.07$	5.94

TABLE 3.5 Activation energy ( $Q$ ) and pre-exponential ( $\rho_0$ ) factors for glass composition no. 3.

Sl. no.	Glass system	$Q \pm \Delta Q$ (eV)	$\rho_0$ (ohm-cm)
1	G3	$0.67 \pm 0.19$	$3 \times 10^{-2}$
2	IG3	$0.49 \pm 0.21$	$2.3 \times 10^{-1}$
3	HIG3	$0.07 \pm 0.04$	3.2

TABLE 3.6 Activation energy ( $Q$ ) and pre-exponential ( $\rho_0$ ) factors for glass composition no. 4

Sl. No.	Glass system	$Q \pm \Delta Q$ (eV)	$\rho_0$ (ohm-cm)
1	G4	$0.73 \pm 0.20$	2.35
2.	IG4	$0.53 \pm 0.22$	14.44
	HIG4	$0.01 \pm 0.007$	$1.64 \times 10^2$

TABLE 3.7 Activation energy ( $Q$ ) and pre-exponential ( $\rho_0$ ) factors for glass composition no. 5.

Sl. No.	Glass system	$Q \pm \Delta Q$ (eV)	$\rho_0$ (ohm-cm)
1	G5	$0.66 \pm 0.23$	$3.4 \times 10^3$
2	IG5	$0.64 \pm 0.17$	$1.32 \times 10^{-3}$
3	HIG5	$-0.001 \pm 0.003$	77.1

of the glass structure ( Mechanical energy) to the activation energy can be neglected. The only barrier to the activation of ions will then be due to electrostatic constraints. In such a situation larger ions ( silver in this case) should have lower activation energies.

In virgin glass systems G the conduction is due to lithium ion migration. So as the lithium content increases the conductivity increases.

The ion exchanged glass systems show further decrease in the value of activation energy and resistivity that is because in ion exchanged systems the majority of conducting species are silver ions and silver ions being larger in size result in further loosening of the network structure and therefore the activation barrier goes further down resulting in higher value of conductivity.

The switching of the ion exchanged glass samples is believed to occur because of the formation of links between disconnected portions of the silver rich phases after ion exchange under the driving force of the suitable combination of electric field and temperature. The growth of the connecting path between silver rich phases takes place because of a lowering of the thermodynamic free energy due to the formation of the such silver-rich phase. The theory of the growth rate has been developed by (Turnbull 1956) according to that expression for growth rate  $U$  is given by :

$$U = \lambda \nu \exp \left( - \frac{\Delta F}{kT} \right) \quad \dots \quad (3.2)$$

where  $\lambda$  is the thickness of one atom layer of the growing phase ,

$\nu$  is the vibrating frequency of the ion ,

$\Delta F$  is the activation energy for ionic diffusion across the interface between the two phases ,

$k$  is the Boltzman constant and ,

$T$  is the absolute temperature .

The equ. 3.2 has been derived under the assumption that inequality  $V/\Delta F_V \gg kT$  holds in the present case where  $V$  is the volume of one ion and  $\Delta F_V$  is the change in free energy per unit volume for the concerned phase transformation .

When the electric field  $E$  is applied the expression for growth rate will be :

$$U_E = \lambda \nu \exp \left[ - \frac{\Delta F}{kT} - \frac{e\lambda E}{kT} \right] \quad \dots \quad (3.3)$$

The critical growth rate at which successive silver-rich regions form a connected high conducting path could be achieved either at a critical electric field  $E_C$  or at a critical temperature  $T_C$ . From equ. 3.2 and 3.3  $E_C$  can be solved to give

$$E_C = \frac{\Delta F}{e \lambda} \left[ 1 - \frac{T}{T_C} \right] \quad \dots \quad (3.4)$$

The decrease in  $E_C$  as a function of  $T$  as predicted by equation 3.4 has been experimentally observed for systems HIG1 and HIG2 (Fig

The dependence is however not linear. This could arise because of the presence of a range of  $\Delta F$  values for the ionic movement from the matrix phase to the product phase. This has been shown to exist for oxide glasses by Taylor(1957).

The very low activation energy in high conducting state of the ion exchanged sample could be explained on the basis of co-operative motion of silver ions in the newly formed interconnected silver rich phase. The large concentrations of silver ions in this state will lead to a state where some of the saddle point positions are also occupied by the silver ions. The ionic transport in such a case arise due to movement of a pair of silver ions ( one in the saddle point position and other in the equilibrium position) together under the influence of the applied electric field giving rise to low activation energy values. The activation energy values and the electrical conductivity values both in unswitched and switched states- are comparable to the values reported in the literature for the fast ion conduction glasses ( Tuller et al 1980) .

The glass composition G2 comprising of 30 mole %  $\text{Li}_2\text{O}$ , 12 mole %  $\text{ZnO}$  and rest  $\text{SiO}_2$  shows a kink in conductivity versus temperature curve. The kink appears around temperature  $T_c = 140^\circ\text{C}$ . The behaviour above  $T_c$  can be explained on the basis of formation of percolating path in several disjointed phases of the two phase microstructure. The conduction is due to lithium ion migration through the connected path thus formed in disconnected portions of the matrix. This explanation however is subjected to confirmation by taking electron micrographs and analysing the two phase

microstructure.

The exact mechanism below  $T_c$  is not clear at this stage. Two possibilities could be envisaged viz.

(i) There is a third interconnected phase in the system having a different structure from that of matrix phase or (ii) Electron or electron-hole conduction due to the presence of  $Zn^{+}$  and  $Zn^{++}$  in this system ( Kingrey) .

### 3.5 POLARIZATION MEASUREMENTS :

The polarization studies have been conducted as discussed in section 2.8. The graphite paint (Polaron Equipment Ltd., England) has been used as blocking electrode on one face of the sample which blocks the ionic conduction as against the silver paint on the other face of the sample which replenishes the silver ions.

The I-V characteristics for  $Ag/HIG/C^{+}$  systems show that the current decreases with time in blocking electrode measurements. This arises because of increase in resistance of sample due to polarization. At first current decreases very rapidly because as soon as the voltage is impressed upon the sample, it gets polarized and further lapse of time does not result in any appreciable polarization of sample and current approaches a constant value.

Figure 3.22 to Figure 3.25 are the I-V characteristics for systems  $Ag/HIG1/C^{+}$ ,  $Ag/HIG2/C^{+}$ ,  $Ag/HIG3/C^{+}$  and  $Ag/HIG4/C^{+}$  respectively and Figure 3.26 to Figure 3.29 are their corresponding current versus time plots.



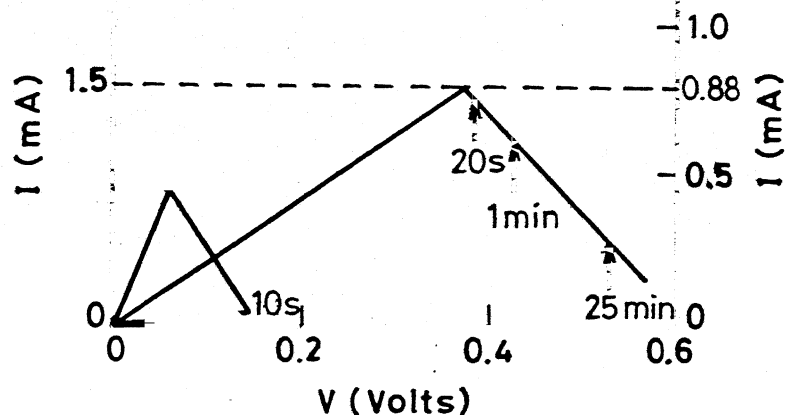


Fig. 3.24 Current-Voltage characteristics for polarization cell Ag/HIG 3/C<sup>+</sup> (T = 26°C)

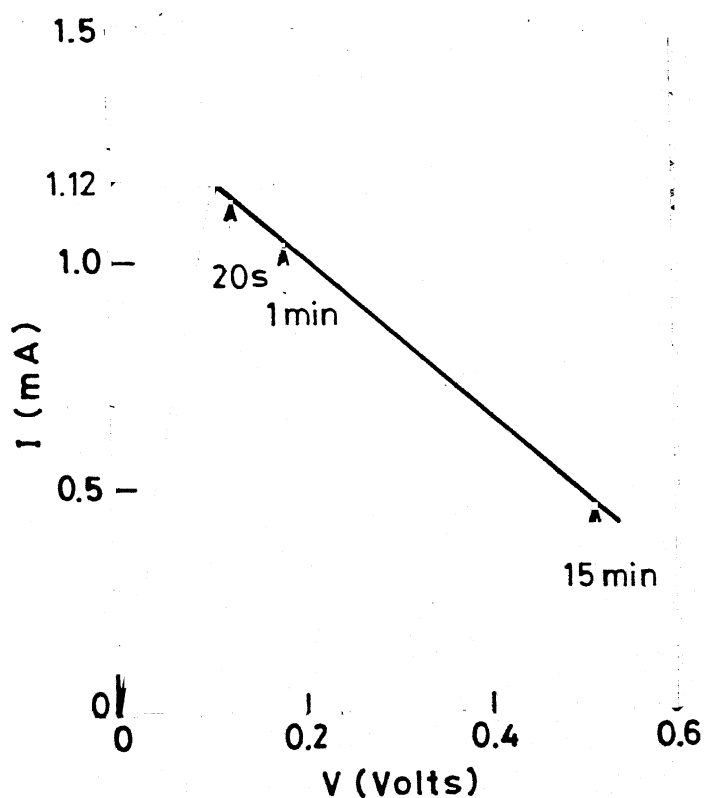


Fig. 3.25 Current-Voltage characteristics for polarization cell Ag/HIG 4/C<sup>+</sup> (T = 27°C)

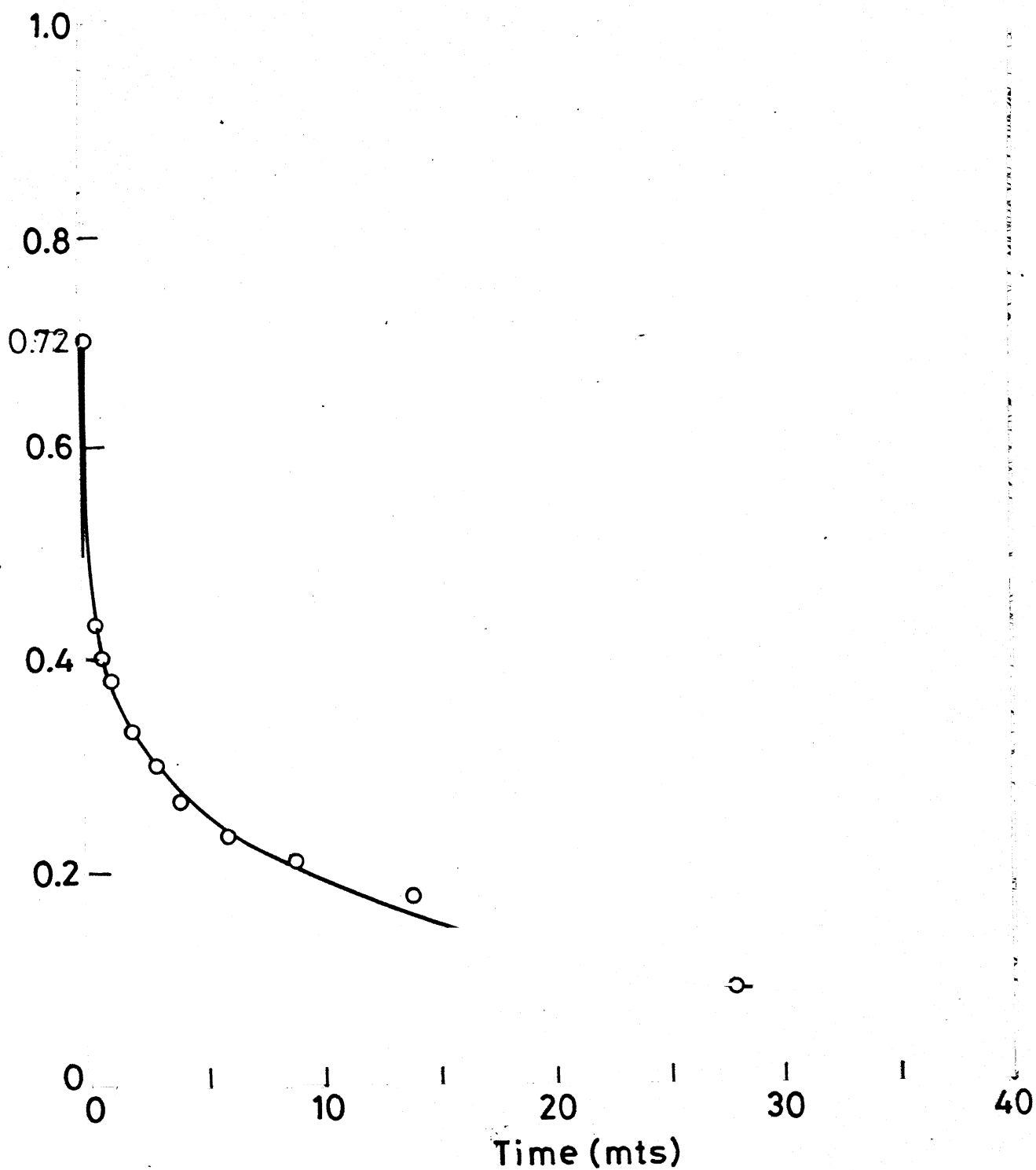


Fig. 3.26 Current as a function of time for system Ag/HIG 1/C<sup>+</sup> (T = 26°C)

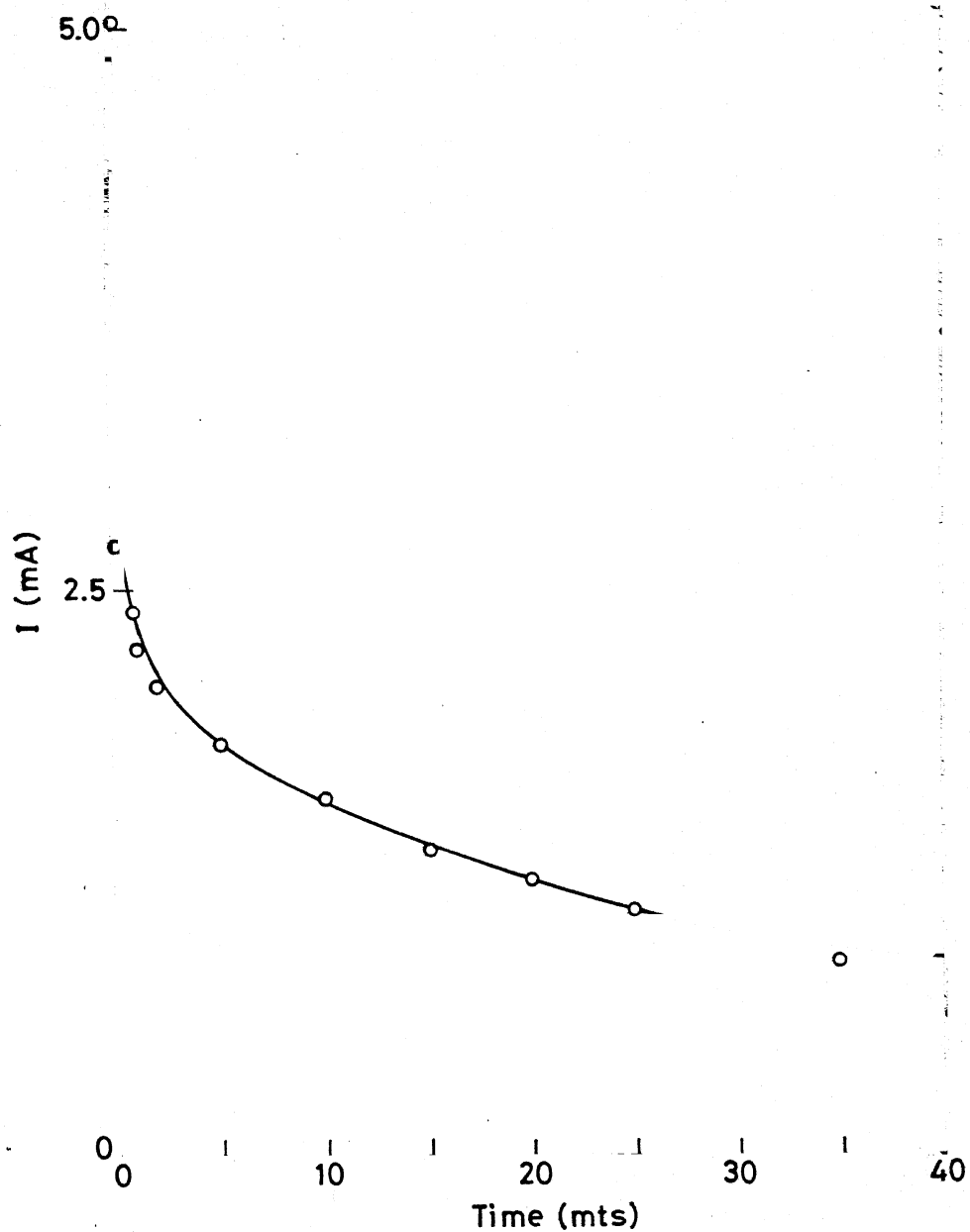


Fig. 3.27 Current as a function of time for system  $\text{Ag/HIG 2/C}^+$  ( $T = 27^\circ\text{C}$ )

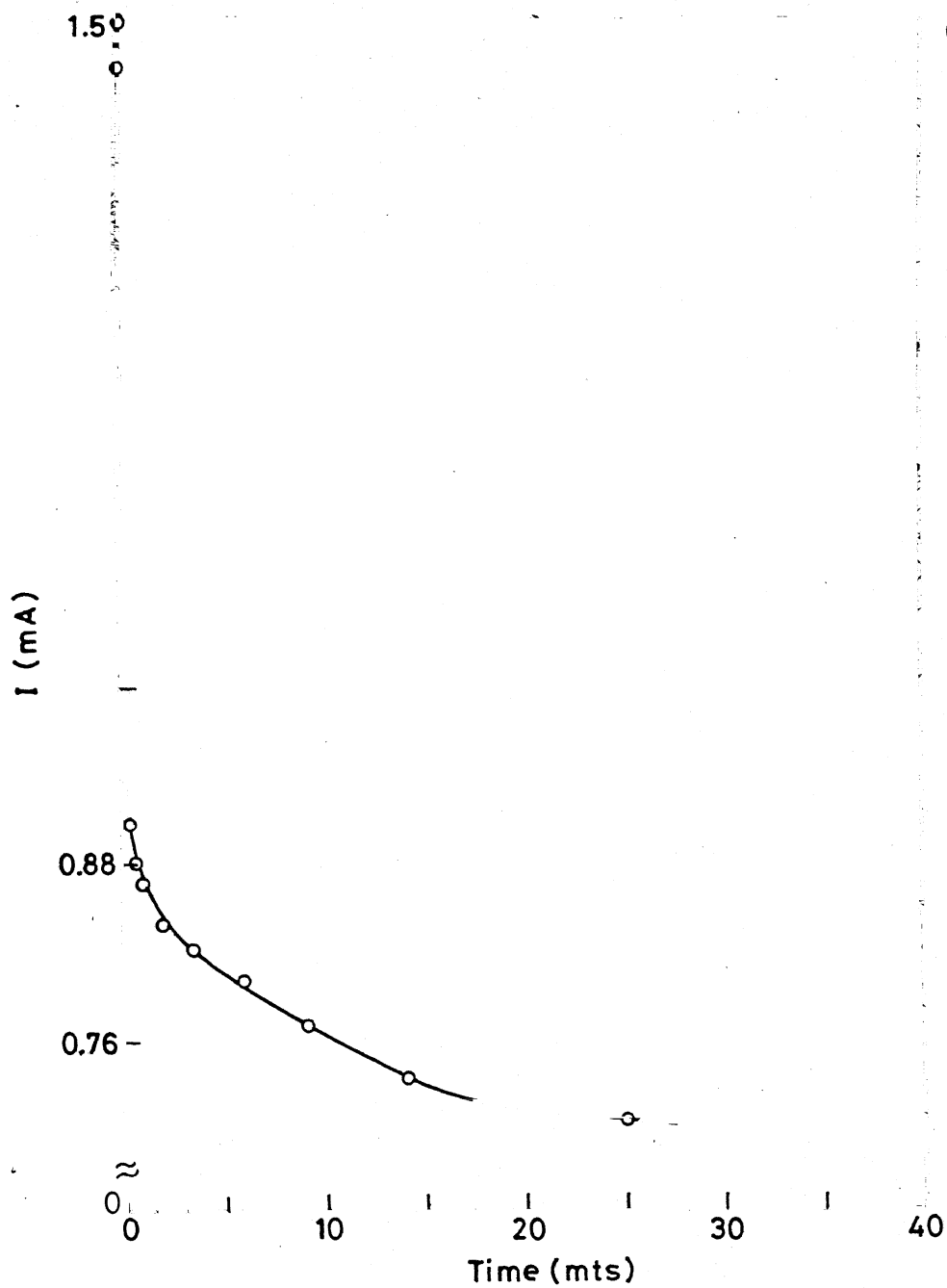


Fig. 3.28 Current as a function of time for system  $\text{Ag/HIG 3/C}^+$  ( $T=26^\circ\text{C}$ ).

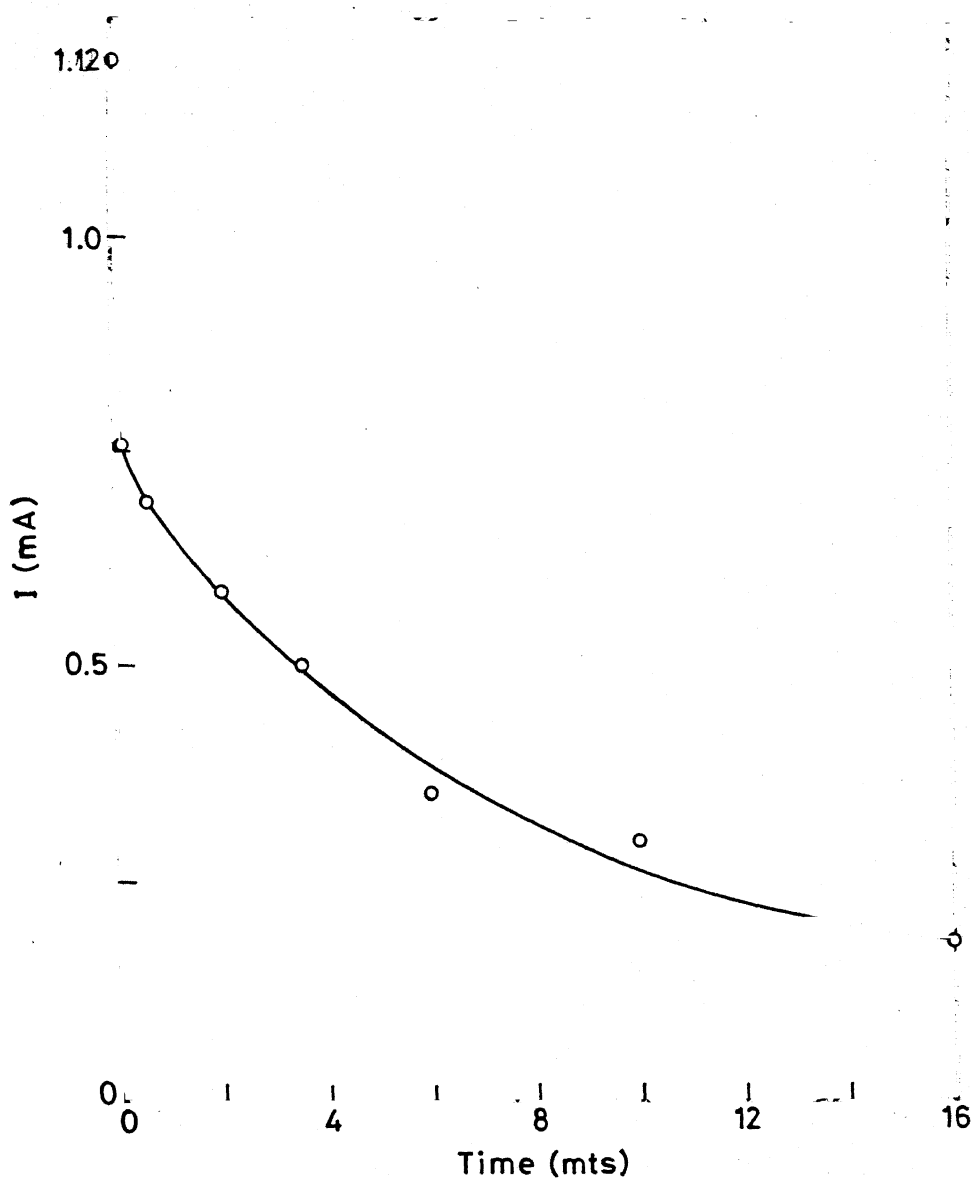


Fig. 3.29 Current as a function of time for system  $\text{Ag/HIG 4/C}^+$  ( $T = 27^\circ\text{C}$ )

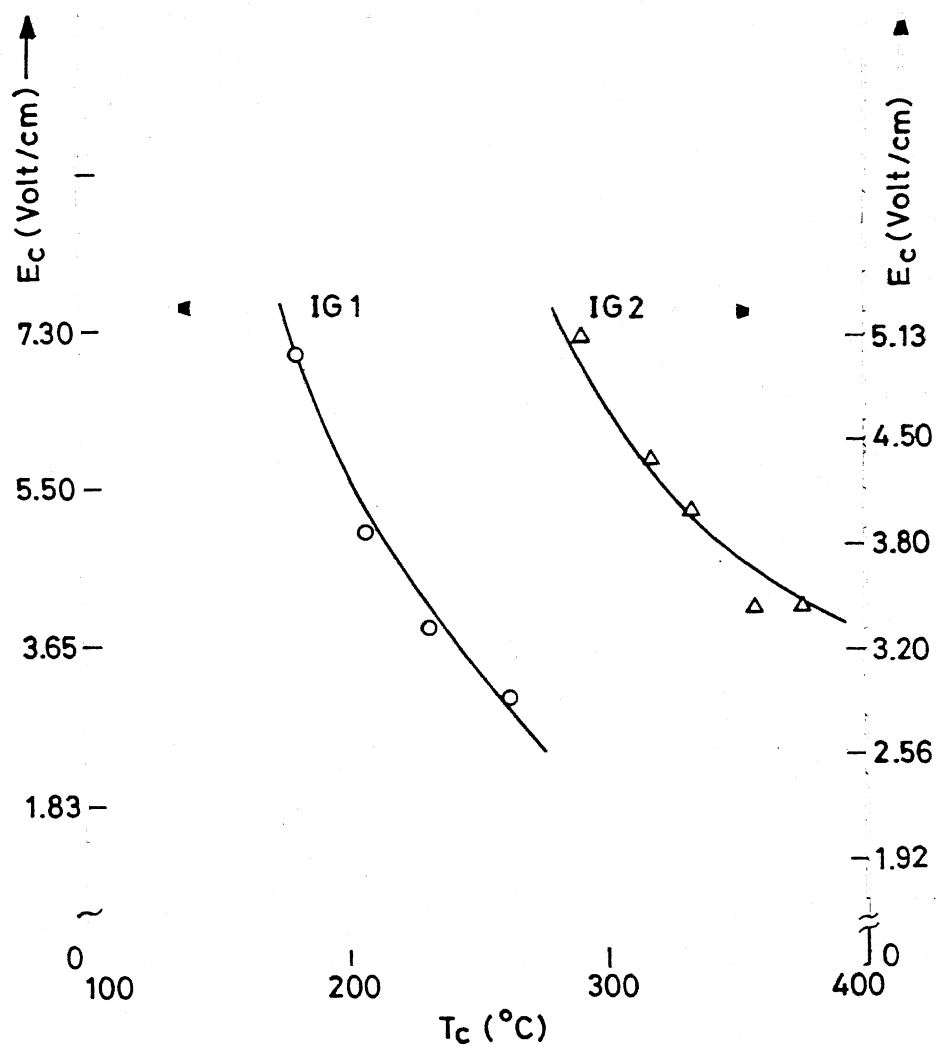


Fig. 3.30 Temperature variation of electric field ( $E_c$ ) for glass system IG1 and IG2.

### 3.5.1 DISCUSSION:

The decrease of current with time "first rapidly and then slowly" for  $\text{Ag/HIG/C}^+$  system for all glass compositions suggests that the ionic conductivity dominates in high conducting state lithium containing silicate glasses and electronic conduction is small since for the electronic conductivity to be dominant the I-V characteristics should not have shown such behaviour. If electronic conductivity is dominant current remains constant in time since the resistance of the circuit ( Fig. 2.3 ) does not change appreciably.

--

## CHAPTER 4

## CONCLUSION AND FUTURE SCOPE OF WORK

From the results of the present investigation the following conclusions may be arrived at:

- 1) The highest conducting glasses are generally AgI based and contain 70-80 mole % of silver ; none of them is silica based. But in the present investigation it has been established that a new class of high conducting glasses which are silica based can be developed by subjecting silica based glasses containing about 30 mole %  $\text{Li}_2\text{O}$  to Lithium silver ion exchange .
- 2) The effect of electric field on the phase morphological change in oxide glasses has been studied by De Vekey and Majumdar 1970. In the present glass systems it appears that the formation of high conducting state is brought about by formation of an interconnected silver-rich phase under the combined influence of temperature and a suitable electric field ( Chakravorty and Shrivastava 1986) .
- 3) The decay of current with time in all the samples in blocking electrode measurement convincingly confirms that in such glass systems conduction is essentially ionic in nature.

The followings are the suggestions for the future work in this area of research.

- 1) The Lithium containing silica based glasses can be subjected to the ion exchange of other metal ions such as copper and the



effect of this treatment on the conductivity can be investigated.

2) The high conducting state in the present glass systems is explained on the basis of formation of an interconnected silver rich phase between disjointed silver rich and silver deficient phases. This filament formation can be investigated by several techniques such as scanning electron microscopy and transmission electron microscopy.

3) The effect of addition of zinc oxide in the lithium containing silicate glasses on the conductivity is not clear at this stage and can be further investigated.

--

## REFERENCES

1. Adler D., Solid State Physics, vol. 21, Eds. Seitz F., Turnbull D. and Ehrenreich H., Academic press, New York, pp. 1 (1968).
2. Anderson P.W., Phys. Rev., 109, 1492 (1958).
3. Armistead W.H., Stookey S.D., 'Photochromic Silicate Glasses Sensitized by Silver Halides', Science, vol. 144, 150-154 (1964).
4. Austin I.G. and Mott N.F., Adv. Phys., 18, 41 (1969).
5. Bockris J.O.M., Kitchener J.A., Sgnatowica S. and Tomlinson J.W., Trans. Faraday Soc., 48, 75 (1952).
6. Chakravorty D., Shjuttleworth A. and Gaskell P.H., J. Mater. Sci., 10, 799 (1972).
7. Chakravorty D. and Shrivastava A., J. Phys. D: Appl. Phys., 19, 2185-2195 (1986).
8. Chandra S., Superionic Solids, Principles and Applications, 17, (North Holland 1981).
9. Charles R.J., J. Appl. Phys., 32, 1115 (1961).
10. Charles R.J., J. Am. Ceram. Soc., 46, 235 (1963).
11. Collins D.R., Schroder D.K. and Sah C.T., Appl. Phys. Lett., 8, 323 (1966).
12. Cohen A.J., 'Mechanism in variable Transmission Silicate Glasses', Proceedings 7th Inter. Congr. Glass.
13. Davis E.A. and Shaw R.F., J. Non-Cryst. Solids, 2, 406 (1970).
14. De Vekey R.C. and Majumdar A.J., Nature, 25, 172 (1970).
15. Frischat G.H. Ionic Diffusion in Oxide Glasses, (Aeder Mannsdorf. Switzerland: Trans. Tech.), 1976.
16. Fritzche H. and Ovshinsky S.R., J. Non-Cryst. Solids, 2, 148 (1970).
17. Geller S., Solid Electrolytes ( Springer-Verlag, 1977).
18. Glass J.M., Nassau K., Negran T.J., J. Appl. Phys., 49 4808 (1978).

19. Grigorovici R., J. Non-Cryst. Solids, 1 , 303 (1969) .
20. Hindley N.K., J. Non-Cryst. Solids, 5, 17 (1971) .
21. Introduction to glass science, Plenum Press, Edited by Pye. L.O., Stevens H.J. and Lacourse W.C.
22. Isard J.O., J. Soc. Glass Tech., 43, 113T (1959) .
23. Isard J.O., Proc. Instn. Elect. Engrs., 109 B No. 22, 440 (1961) .
24. Kingrey W.D., Introduction to ceramics, John Wiley and Sons, New York (1960) .
25. Kinser D.L. Hench L.L., J. Am. Ceram. Soc., 52, 173 (1960) .
26. Kreidl N.J., Blair G.E., A System of megaorentgen Glass Dosimetry, 45 [1] 56-60 (1956) .
27. Levasseur A., Cales-B, Reau J., and Hangen Muller, P., Mat. Res. Bull., 13, 205 (1978) .
28. Leroy D., Lucas J., Poulain M. and Ravaine D., Mat. Res. Bull., 13, 1125 (1978) .
29. Mackenzie, Ibid.,pg. 126.
30. Minami T., Takuma Y. and Tanaka M., J. Electrochem. Soc., 124, 1659 (1977) .
31. Moore H., Dilva R.C., J. Soc. Glass Tech., 36, 5T (1952) .
32. Mott N.F., Adv. Phys., 16, 49 (1967) .
33. Owen A.E. and Douglas R.W., J. Soc Glass Tech., 43, 159T (1959) .
34. Owen, A.E., Progress in ceramic science, vol. 3, Pergamon press, N.Y., Ed. By Burke J., 77 (1963) .
35. Pearson A.D., Pg. 29 in modern aspects of the vitreous state, vol. 3, Ed. Mackenzie J.D., Butterworths, Washington (1964) .
36. Pearson A.D., J. Non-Cryst. Solids, 2, 1 (1970) .
37. Proctor T.M., and Sutton P.M., J. Am. Ceram. Soc., 43 173 (1960) .
38. Pollack M. and Geballe T.H., Phys. Rev., 122,1742 (1961) .

39. Rawson H., Properties and applications of glass, (Amsterdam: Elsevier), 1984.
40. Riebling E.F., J. Chem. Phys., 55, 804 (1971).
41. Salamon M.B., 'Physics of super ionic conductors' Ed. by Salamon M.B., Springer-Verlag, Berlin, pp. 1-3 (1979).
42. Seddon E., Tippet E., Turner, W., J. Soc. Glass Tech., 16, 450T (1932).
43. Shahi K., Phys. State. Solidi (a), 41, 11-44 (1977).
44. Smedley S.I. and Angell C.A., Sol. State Comm., 27, (1978).
45. Smith G.P., 'Photochromic Silver Hallide Glasses', Proceedings 7th International Congr. Glass.
46. Snitzer E., 'Glass Lasers', Glass industry, 48, 498-503 (1967).
47. Stevels J.M., Electrical property of Glasses in Handbuch der Physik vol. XX, Ed. by Flugge S.W. (Berlin : Springer), 350 (1957).
48. Sudworth J.L., J. Power Sources, 11, 143 (1984).
49. Tanaka K., Lizima S., Sugi M. and Kikuchi M., Solid State Commun., 8, 75 (1970).
50. Taylor H.E., Trans. Farad. Soc., 52 873 (1956).
51. Taylor H.E., J. Soc. Glass Tech., 14, 350 (1957).
52. Tickle R.E., Phys. Chem. Glasses, 8, 101 (1967).
53. Tuller H.L., Button D.P. and Uhlmann D.R., J. Non-Cryst. Solids, 40, 93 (1980).
54. Turnbull D., Phase Transformations, Solid state physics, vol. 3, ( New York: Academic Press ) 1956.
55. Warburg G., Ann. Phys., 21, 622 (1984).
56. Yao Y.F. Y. and Kummer J.T., J. Inorg. Nucl. Chem., 29, 2453 (1967).